

New Directions in Quantum Chromodynamics*

Stanley J. Brodsky

Stanford Linear Accelerator Center

Stanford University, Stanford, California 94309

Abstract

I review the light-cone Fock state representation and its associated light-cone factorization scheme as a method for encoding the flavor, momentum, and helicity properties of hadrons in the form of universal process-independent and frame-independent amplitudes. Discrete light-cone quantization (DLCQ) provides a matrix representation of the QCD Hamiltonian and a nonperturbative method for computing the quark and gluon bound state wavefunctions. A number of applications of the light-cone formalism are discussed, including an exact light-cone Fock state representation of semi-leptonic B decay amplitudes. Hard exclusive and diffractive reactions are shown to be sensitive to hadron distribution amplitudes, the valence Fock state hadronic wavefunctions at small impact separation. Semi-exclusive reactions are shown to provide new flavor-dependent probes of distribution amplitudes and new types of deep inelastic currents. “Self-resolving” diffractive processes and Coulomb dissociation are discussed as a direct measure of the light-cone wavefunctions of hadrons. Alternatively, one can use Coulomb dissociation to resolve nuclei in terms of their nucleonic and mesonic degrees of freedom. I also discuss several theoretical tools which eliminate theoretical ambiguities in perturbative QCD predictions. For example, commensurate scale relations are perturbative QCD predictions based on conformal symmetry which relate observable to observable at fixed relative scale; such relations have no renormalization scale or scheme ambiguity. I also discuss the utility of the α_V coupling, defined from the QCD heavy quark potential, as a useful physical expansion parameter for perturbative QCD and grand unification. New results on the analytic fermion masses dependence of the α_V coupling at two-loop order are presented.

*Invited talk presented at
International Summer School on Particle Production Spanning MeV and TeV
Energies (Nijmegen 99)
Nijmegen, The Netherlands
8–20 August 1999*

*Work supported by Department of Energy contract DE-AC03-76SF00515.

1 Introduction

In quantum chromodynamics, hadrons are identified as relativistic color-singlet bound states of confined quarks and gluons. A primary goal of high energy and nuclear physics is to unravel the nonperturbative structure and dynamics of nucleons and nuclei in terms of their fundamental quark and gluon degrees of freedom. QCD is a relativistic quantum field theory, so that a fundamental description of hadrons must be at the amplitude level. Part of the complexity of hadronic physics is related to the fact that the eigensolutions of a relativistic theory fluctuate not only in momentum space and helicity, but also in particle number. For example, the heavy quark sea of the proton is associated with higher particle number Fock states. Thus any wavefunction description must allow for arbitrary fluctuations in particle number.

Since the discovery of Bjorken scaling [1] of deep inelastic lepton-proton scattering in 1969 [2], high energy experiment have provided an extraordinary amount of information on the flavor, momentum, and helicity distributions of the quark and gluon in hadrons. This information is generally encoded in the leading twist factorized quark and gluon distributions $q_{\lambda_q, \lambda_N}(x, Q)$, $g_{\lambda_g, \lambda_N}(x, Q)$. However, since such distributions are single-particle probabilities, they contain no information on the transverse momentum distributions, multiparticle flavor and helicity correlations, or quantum mechanical phases, information critical to understanding higher twist processes or exclusive processes such as form factors, elastic scattering, and the exclusive decays of heavy hadrons. Although it is convenient for computational reasons to separate hard, perturbatively calculable, and soft non-perturbative physics, the theory has no such intrinsic division. The analysis of QCD processes at the amplitude level is a challenging relativistic many-body problem, mixing issues involving confinement, chiral symmetry, non-perturbative and perturbative dynamics, and thus a theoretical complexity far beyond traditional bound state problems.

Deep inelastic lepton-proton scattering has provided the traditional guide to hadron structure. The focus in high energy physics has been on the logarithmic DGLAP evolution of the structure functions and the associated jet structure as a test of perturbative QCD. However, when the photon virtuality is small and of order of the quark intrinsic transverse momentum, evolution from QCD radiative processes becomes quenched, and the structure functions reveal fundamental features of the proton's

composition. The deep inelastic scattering data in fact show that the nonperturbative structure of nucleons is more complex than suggested by a three-quark bound state. For example, if the sea quarks were generated solely by perturbative QCD evolution via gluon splitting, the anti-quark distributions would be approximately isospin symmetric. However, the $\bar{u}(x)$ and $\bar{d}(x)$ antiquark distributions of the proton at $Q^2 \sim 10 \text{ GeV}^2$ are found to be quite different in shape [3] and thus must reflect dynamics intrinsic to the proton's structure. Evidence for a difference between the $\bar{s}(x)$ and $s(x)$ distributions has also been claimed [4]. There have also been surprises associated with the chirality distributions $\Delta q = q_{\uparrow/\uparrow} - q_{\downarrow/\uparrow}$ of the valence quarks which show that a simple valence quark approximation to nucleon spin structure functions is far from the actual dynamical situation [5].

It is helpful to categorize the parton distributions as “intrinsic”—pertaining to the long-time scale composition of the target hadron, and “extrinsic”,—reflecting the short-time substructure of the individual quarks and gluons themselves. Gluons carry a significant fraction of the proton's spin as well as its momentum. Since gluon exchange between valence quarks contributes to the $p - \Delta$ mass splitting, it follows that the gluon distributions cannot be solely accounted for by gluon bremsstrahlung from individual quarks, the process responsible for DGLAP evolutions of the structure functions. Similarly, in the case of heavy quarks, $s\bar{s}$, $c\bar{c}$, $b\bar{b}$, the diagrams in which the sea quarks are multiply connected to the valence quarks are intrinsic to the proton structure itself [6]. The x distribution of intrinsic heavy quarks is peaked at large x reflecting the fact that higher Fock state wavefunctions containing heavy quarks are maximal when the off-shellness of the fluctuation is minimized. The evidence for intrinsic charm at large x in deep inelastic scattering is discussed by Harris *et al.*[7] Thus neither gluons nor sea quarks are solely generated by DGLAP evolution, and one cannot define a resolution scale Q_0 where the sea or gluon degrees of freedom can be neglected.

In these lectures, I shall emphasize the utility of light-cone Hamiltonian quantization and the light-cone Fock wavefunctions for representing hadrons in terms of their quark and gluon degrees of freedom. The fundamental eigenvalue problem of QCD takes the form of a Heisenberg equation:

$$H_{LC}^{QCD} |\Psi_H\rangle = M_H^2 |\Psi_H\rangle \quad (1)$$

where the theory is quantized at fixed light-cone “time” $\tau = t + z/c$ [8]. This representation is the extension of Schrödinger many-body theory to the relativistic domain. The eigenvalues of the light-cone Hamiltonian H_{LC}^{QCD} is the square of the hadron masses M_H , the discrete spectrum as well as the bound states. Each eigenfunction can be decomposed on the complete basis of eigensolutions $|n\rangle$ of the free Hamiltonian $H_{LC}^0 = H_{LC}^{QCD}(g \rightarrow 0)$. The light-cone Fock projections of the eigensolution

$$\psi_{n/H}(x_i, \vec{k}_{\perp i}, \lambda_i) = \langle n(x_i, k_{\perp i}, \lambda_i) | \Psi_H \rangle, i = 1 \cdots n \quad (2)$$

encode all of the information of the hadron in terms of the flavor, helicity, and momentum content of its quark and gluon constituents. For example, the proton state has the Fock expansion

$$\begin{aligned} |p\rangle &= \sum_n \langle n | p \rangle |n\rangle \\ &= \psi_{3q/p}^{(\Lambda)}(x_i, \vec{k}_{\perp i}, \lambda_i) |uud\rangle \\ &\quad + \psi_{3qg/p}^{(\Lambda)}(x_i, \vec{k}_{\perp i}, \lambda_i) |uudg\rangle + \cdots \end{aligned} \quad (3)$$

representing the expansion of the exact QCD eigenstate on a non-interacting quark and gluon basis. The probability amplitude for each such n -particle state of on-mass shell quarks and gluons in a hadron is given by a light-cone Fock state wavefunction $\psi_{n/H}(x_i, \vec{k}_{\perp i}, \lambda_i)$, where the constituents have longitudinal light-cone momentum fractions $x_i = k_i^+ / p^+ = (k_i^0 + k_i^z) / (p^0 + p^z)$, $\sum_{i=1}^n x_i = 1$, relative transverse momentum $\vec{k}_{\perp i}$, $\sum_{i=1}^n \vec{k}_{\perp i} = \vec{0}_{\perp}$, and helicities λ_i .

The light-cone Fock formalism is derived in the following way: one first constructs the light-cone time evolution operator $P^- = P^0 - P^z$ and the invariant mass operator $H_{LC} = P^- P^+ - P_{\perp}^2$ in light-cone gauge $A^+ = 0$ from the QCD Lagrangian. The dependent field theoretic degrees of freedom are eliminated using the QCD equations of motion. The total longitudinal momentum $P^+ = P^0 + P^z$ and transverse momenta \vec{P}_{\perp} are conserved, *i.e.* are independent of the interactions. The P^- light-cone evolution operator is constructed from the independent field theoretic degrees of freedom. The matrix elements of H_{LC} on the complete orthonormal basis $\{|n\rangle\}$ of the free theory $H_{LC}^0 = H_{LC}(g = 0)$ can then be constructed. The matrix elements $\langle n | H_{LC} | m \rangle$ connect Fock states differing by 0, 1, or 2 quark or gluon quanta, and they include the instantaneous quark and gluon contributions imposed by eliminating dependent degrees of freedom in light-cone gauge.

The LC wavefunctions $\psi_{n/H}(x_i, \vec{k}_{\perp i}, \lambda_i)$ are universal, process independent, and thus control all hadronic reactions. For example, the quark distributions measured in hard inclusive reactions are

$$q_{\lambda_q/\lambda_p}(x, \Lambda) = \sum_{n, q_a} \int \prod_{j=1}^n dx_j d^2 k_{\perp j} \sum_{\lambda_i} |\psi_{n/H}^{(\Lambda)}(x_i, \vec{k}_{\perp i}, \lambda_i)|^2 \quad (4)$$

$$\times \delta\left(1 - \sum_i x_i\right) \delta^{(2)}\left(\sum_i \vec{k}_{\perp i}\right) \delta(x - x_q) \delta_{\lambda_a, \lambda_q} \Theta(\Lambda^2 - \mathcal{M}_n^2)$$

where the sum is over all quarks q_a which match the quantum numbers, light-cone momentum fraction x and helicity of the probe quark. The effective lifetime of each configuration in the laboratory frame is $2P_{\text{lab}}/(\mathcal{M}_n^2 - M_p^2)$ where $\mathcal{M}_n^2 = \sum_{i=1}^n (k_{\perp i}^2 + m_i^2)/x_i < \Lambda^2$ is the off-shell invariant mass and Λ is a global ultraviolet regulator. The light-cone momentum integrals are thus limited by requiring that the invariant mass squared of the constituents of each Fock state is less than the resolution scale Λ . This cutoff serves to define a factorization scheme for separating hard and soft regimes in both exclusive and inclusive hard scattering reactions.

A crucial feature of the light-cone formalism is the fact that the form of the $\psi_{n/H}^{(\Lambda)}(x_i, \vec{k}_{\perp i}, \lambda_i)$ is invariant under longitudinal boosts; *i.e.*, the light-cone wavefunctions expressed in the relative coordinates x_i and $k_{\perp i}$ are independent of the total momentum P^+ , \vec{P}_{\perp} of the hadron. The ensemble $\{\psi_{n/H}\}$ of such light-cone Fock wavefunctions is a key concept for hadronic physics, providing a conceptual basis for representing physical hadrons (and also nuclei) in terms of their fundamental quark and gluon degrees of freedom. Each Fock state interacts distinctly; *e.g.*, Fock states with small particle number and small impact separation have small color dipole moments and can traverse a nucleus with minimal interactions. This is the basis for the predictions for “color transparency” [9].

Given the $\psi_{n/H}^{(\Lambda)}$, one can construct any spacelike electromagnetic or electroweak form factor from the diagonal overlap of the LC wavefunctions [10]. The natural formalism for describing the hadronic wavefunctions which enter exclusive and diffractive amplitudes is the light-cone expansion. Similarly, the matrix elements of the currents that define quark and gluon structure functions can be computed from the integrated squares of the LC wavefunctions [11].

Factorization theorems for hard exclusive, semi-exclusive, and diffractive processes allow a rigorous separation of soft non-perturbative dynamics of the bound state

hadrons from the hard dynamics of a perturbatively-calculable quark-gluon scattering amplitude.

Roughly, the direct proofs of factorization in the light-cone scheme proceed as follows: In hard inclusive reactions all intermediate states are divided according to $\mathcal{M}_n^2 < \Lambda^2$ and $\mathcal{M}_n^2 > \Lambda^2$ domains. The lower region is associated with the quark and gluon distributions defined from the absolute squares of the LC wavefunctions in the light cone factorization scheme. In the high invariant mass regime, intrinsic transverse momenta can be ignored, so that the structure of the process at leading power has the form of hard scattering on collinear quark and gluon constituents, as in the parton model. The attachment of gluons from the LC wavefunction to a propagator in the hard subprocess is power-law suppressed in LC gauge, so that the minimal $2 \rightarrow 2$ quark-gluon subprocesses dominate. The higher order loop corrections lead to the DGLAP evolution equations.

It is important to note that the effective starting point for the PQCD evolution of the structure functions cannot be taken as a constant Q_0^2 since as $x \rightarrow 1$ the invariant mass \mathcal{M}_n exceeds the resolution scale Λ . Thus in effect, evolution is quenched at $x \rightarrow 1$. The anomaly contribution to singlet helicity structure function $g_1(x, Q)$ can be explicitly identified in the LC factorization scheme as due to the $\gamma^* g \rightarrow q\bar{q}$ fusion process. The anomaly contribution would be zero if the gluon is on shell. However, if the off-shellness of the state is larger than the quark pair mass, one obtains the usual anomaly contribution [12].

In exclusive amplitudes, the LC wavefunctions are the interpolating functions between the quark and gluon states and the hadronic states. In an exclusive amplitude involving a hard scale Q^2 all intermediate states can be divided according to $\mathcal{M}_n^2 < \Lambda^2 < Q^2$ and $\mathcal{M}_n^2 > \Lambda^2$ invariant mass domains. The high invariant mass contributions to the amplitude has the structure of a hard scattering process T_H in which the hadrons are replaced by their respective (collinear) quarks and gluons. In light-cone gauge only the minimal Fock states contribute to the leading power-law fall-off of the exclusive amplitude. The wavefunctions in the lower invariant mass domain can be integrated up to the invariant mass cutoff Λ and replaced by the gauge invariant distribution amplitudes, $\phi_H(x_i, \Lambda)$. Final state and initial state corrections from gluon attachments to lines connected to the color-singlet distribution amplitudes cancel at leading twist.

Thus the key non-perturbative input for exclusive processes is the gauge and frame independent hadron distribution amplitude [11] defined as the integral of the valence (lowest particle number) Fock wavefunction; *e.g.* for the pion

$$\phi_\pi(x_i, \Lambda) \equiv \int d^2k_\perp \psi_{q\bar{q}/\pi}^{(\Lambda)}(x_i, \vec{k}_\perp, \lambda) \quad (5)$$

where the global cutoff Λ is identified with the resolution Q . The distribution amplitude controls leading-twist exclusive amplitudes at high momentum transfer, and it can be related to the gauge-invariant Bethe-Salpeter wavefunction at equal light-cone time $\tau = x^+$. The logarithmic evolution of hadron distribution amplitudes $\phi_H(x_i, Q)$ can be derived from the perturbatively-computable tail of the valence light-cone wavefunction in the high transverse momentum regime [11]. Further details are provided in the following sections.

The existence of an exact formalism provides a basis for systematic approximations and a control over neglected terms. For example, one can analyze exclusive semi-leptonic B -decays which involve hard internal momentum transfer using a perturbative QCD formalism [13, 14] patterned after the analysis of form factors at large momentum transfer [11]. The hard-scattering analysis proceeds by writing each hadronic wavefunction as a sum of soft and hard contributions

$$\psi_n = \psi_n^{\text{soft}}(\mathcal{M}_n^2 < \Lambda^2) + \psi_n^{\text{hard}}(\mathcal{M}_n^2 > \Lambda^2), \quad (6)$$

where \mathcal{M}_n^2 is the invariant mass of the partons in the n -particle Fock state and Λ is the separation scale. The high internal momentum contributions to the wavefunction ψ_n^{hard} can be calculated systematically from QCD perturbation theory by iterating the gluon exchange kernel. Again, the contributions from high momentum transfer exchange to the B -decay amplitude can then be written as a convolution of a hard-scattering quark-gluon scattering amplitude T_H with the distribution amplitudes $\phi(x_i, \Lambda)$, the valence wavefunctions obtained by integrating the constituent momenta up to the separation scale $\mathcal{M}_n < \Lambda < Q$. This is the basis for the perturbative hard-scattering analyses [13, 15, 16, 14]. In the exact analysis, one can identify the hard PQCD contribution as well as the soft contribution from the convolution of the light-cone wavefunctions. Furthermore, the hard-scattering contribution can be systematically improved.

It is thus important to not only compute the spectrum of hadrons and gluonic states, but also to determine the wavefunction of each QCD bound state in terms of

its fundamental quark and gluon degrees of freedom. If we could obtain such nonperturbative solutions of QCD, then we could compute the quark and gluon structure functions and distribution amplitudes which control hard-scattering inclusive and exclusive reactions as well as calculate the matrix elements of currents which underlie electroweak form factors and the weak decay amplitudes of the light and heavy hadrons. The light-cone wavefunctions also determine the multi-parton correlations which control the distribution of particles in the proton fragmentation region as well as dynamical higher twist effects. Thus one can analyze not only the deep inelastic structure functions but also the fragmentation of the spectator system. Knowledge of hadron wavefunctions would also open a window to a deeper understanding of the physics of QCD at the amplitude level, illuminating exotic effects of the theory such as color transparency, intrinsic heavy quark effects, hidden color, diffractive processes, and the QCD van der Waals interactions.

Can we ever hope to compute the light-cone wavefunctions from first principles in QCD? In the Discretized Light-Cone Quantization (DLCQ) method [17], periodic boundary conditions are introduced in order to render the set of light-cone momenta $k_i^+, k_{\perp i}$ discrete. Solving QCD then becomes reduced to diagonalizing the mass operator of the theory. Virtually any 1+1 quantum field theory, including “reduced QCD” (which has both quark and gluonic degrees of freedom) can be completely solved using DLCQ [18, 19]. The method yields not only the bound-state and continuum spectrum, but also the light-cone wavefunction for each eigensolution. The method is particularly elegant in the case of supersymmetric theories [20]. The solutions for the model 1+1 theories can provide an important theoretical laboratory for testing approximations and QCD-based models. Recent progress in DLCQ has been obtained for 3+1 theories utilizing Pauli-Villars ghost fields to provide a covariant regularization. Broken supersymmetry may be the key method for regulating non-Abelian theories. Light-cone gauge $A^+ = 0$ allows one to utilize only the physical degrees of freedom of the gluon field. However, light-cone quantization in Feynman gauge has a number of attractive features, including manifest covariance and a straightforward passage to the Coulomb limit in the case of static quarks [21].

Light-cone wavefunctions thus are the natural quantities to encode hadron properties and to bridge the gap between empirical constraints and theoretical predictions for the bound state solutions. We can thus envision a program to construct the hadronic

light cone Fock wavefunctions $\psi_n(x_i, k_{\perp i}, \lambda_i)$ using not only data but constraints such as:

(1) Since the state is far off shell at large invariant mass \mathcal{M} , one can derive rigorous limits on the $x \rightarrow 1$, high k_{\perp} , and high \mathcal{M}_n^2 behavior of the wavefunctions in the perturbative domain.

(2) Ladder relations connecting state of different particle number follow from the QCD equation of motion and lead to Regge behavior of the quark and gluon distributions at $x \rightarrow 0$. QED provides a constraint at $N_C \rightarrow 0$.

(3) One can obtain guides to the exact behavior of LC wavefunctions in QCD from analytic or DLCQ solutions to toy models such as “reduced” $QCD(1+1)$.

(4) QCD sum rules, lattice gauge theory moments, and QCD inspired models such as the bag model, chiral theories, provide important constraints.

(5) Since the LC formalism is valid at all scales, one can utilize empirical constraints such as the measurements of magnetic moments, axial couplings, form factors, and distribution amplitudes.

(6) In the nonrelativistic limit, the light-cone and many-body Schrödinger theory formalisms must match.

In addition to the light-cone Fock expansion, a number of other useful theoretical tools are available to eliminate theoretical ambiguities in QCD predictions:

(1) Conformal symmetry provides a template for QCD predictions, leading to relations between observables which are present even in a theory which is not scale invariant. For example, the natural representation of distribution amplitudes is in terms of an expansion of orthonormal conformal functions multiplied by anomalous dimensions determined by QCD evolution equations [22, 23]. Thus an important guide in QCD analyses is to identify the underlying conformal relations of QCD which are manifest if we drop quark masses and effects due to the running of the QCD couplings. In fact, if QCD has an infrared fixed point (vanishing of the Gell Mann-Low function at low momenta), the theory will closely resemble a scale-free conformally symmetric theory in many applications.

(2) Commensurate scale relations [24] are perturbative QCD predictions which relate observable to observable at fixed relative scale, such as the “generalized Crewther relation” [25], which connects the Bjorken and Gross-Llewellyn Smith deep inelastic scattering sum rules to measurements of the e^+e^- annihilation cross section. The

relations have no renormalization scale or scheme ambiguity. The coefficients in the perturbative series for commensurate scale relations are identical to those of conformal QCD; thus no infrared renormalons are present [26]. One can identify the required conformal coefficients at any finite order by expanding the coefficients of the usual PQCD expansion around a formal infrared fixed point, as in the Banks-Zak method [27]. All non-conformal effects are absorbed by fixing the ratio of the respective momentum transfer and energy scales. In the case of fixed-point theories, commensurate scale relations relate both the ratio of couplings and the ratio of scales as the fixed point is approached [26].

(3) α_V Scheme. A natural scheme for defining the QCD coupling in exclusive and other processes is the $\alpha_V(Q^2)$ scheme defined from the potential of static heavy quarks. Heavy-quark lattice gauge theory can provide highly precise values for the coupling. All vacuum polarization corrections due to fermion pairs are then automatically and analytically incorporated into the Gell Mann-Low function, thus avoiding the problem of explicitly computing and resumming quark mass corrections related to the running of the coupling. The use of a finite effective charge such as α_V as the expansion parameter also provides a basis for regulating the infrared nonperturbative domain of the QCD coupling.

(4) The Abelian Correspondence Principle. One can consider QCD predictions as analytic functions of the number of colors N_C and flavors N_F . In particular, one can show at all orders of perturbation theory that PQCD predictions reduce to those of an Abelian theory at $N_C \rightarrow 0$ with $\hat{\alpha} = C_F \alpha_s$ and $\hat{N}_F = N_F / TC_F$ held fixed [28]. There is thus a deep connection between QCD processes and their corresponding QED analogs.

2 Discretized Light-Cone Quantization

Solving a quantum field theory such as QCD is clearly not easy. However, highly nontrivial, one-space one-time relativistic quantum field theories which mimic many of the features of QCD, have already been completely solved using light-cone Hamiltonian methods [8]. Virtually any (1+1) quantum field theory can be solved using the method of Discretized Light-Cone-Quantization (DLCQ) [17, 29] where the matrix elements $\langle n | H_{LC}^\Lambda | m \rangle$, are made discrete in momentum space by imposing periodic

or anti-periodic boundary conditions in $x^- = x^0 - x^z$ and \vec{x}_\perp . Upon diagonalization of H_{LC} , the eigenvalues provide the invariant mass of the bound states and eigenstates of the continuum. In DLCQ, the Hamiltonian H_{LC} , which can be constructed from the Lagrangian using light-cone time quantization, is completely diagonalized, in analogy to Heisenberg's solution of the eigenvalue problem in quantum mechanics. The quantum field theory problem is rendered discrete by imposing periodic or anti-periodic boundary conditions. The eigenvalues and eigensolutions of collinear QCD then give the complete spectrum of hadrons, nuclei, and gluonium and their respective light-cone wavefunctions. A beautiful example is "collinear" QCD: a variant of $QCD(3 + 1)$ defined by dropping all of interaction terms in H_{LC}^{QCD} involving transverse momenta [18]. Even though this theory is effectively two-dimensional, the transversely-polarized degrees of freedom of the gluon field are retained as two scalar fields. Antonuccio and Dalley [19] have used DLCQ to solve this theory. The diagonalization of H_{LC} provides not only the complete bound and continuum spectrum of the collinear theory, including the gluonium states, but it also yields the complete ensemble of light-cone Fock state wavefunctions needed to construct quark and gluon structure functions for each bound state. Although the collinear theory is a drastic approximation to physical $QCD(3 + 1)$, the phenomenology of its DLCQ solutions demonstrate general gauge theory features, such as the peaking of the wavefunctions at minimal invariant mass, color coherence and the helicity retention of leading partons in the polarized structure functions at $x \rightarrow 1$. The solutions of the quantum field theory can be obtained for arbitrary coupling strength, flavors, and colors.

In practice it is essential to introduce an ultraviolet regulator in order to limit the total range of $\langle n | H_{LC} | m \rangle$, such as the "global" cutoff in the invariant mass of the free Fock state. One can also introduce a "local" cutoff to limit the change in invariant mass $|\mathcal{M}_n^2 - \mathcal{M}_m^2| < \Lambda_{\text{local}}^2$ which provides spectator-independent regularization of the sub-divergences associated with mass and coupling renormalization. Recently, Hiller, McCartor, and I have shown [30] that the Pauli-Villars method has advantages for regulating light-cone quantized Hamiltonian theory. A spectrum of Pauli-Villars ghost fields satisfying three spectral conditions will regulate the interactions in the ultraviolet, while at same time avoiding spectator-dependent renormalization and preserving chiral symmetry. We have also shown that model theories in $3+!$ dimensions can be successfully solved with such regularization.

Although gauge theories are usually quantized on the light-cone in light-cone gauge $A^+ = 0$, it is also possible and interesting to quantize the theory in Feynman gauge [21]. Covariant gauges are advantageous since they preserve the rotational symmetry of the gauge interactions.

The natural renormalization scheme for the QCD coupling is $\alpha_V(Q)$, the effective charge defined from the scattering of two infinitely-heavy quark test charges. This is discussed in more detail below. The renormalization scale can then be determined from the virtuality of the exchanged momentum, as in the BLM and commensurate scale methods [31, 24, 25, 32]. Similar effective charges have been proposed by Watson [33] and Czarnecki *et al.*[34]

In principle, we could also construct the wavefunctions of QCD(3+1) starting with collinear QCD(1+1) solutions by systematic perturbation theory in ΔH , where ΔH contains the terms which produce particles at non-zero k_\perp , including the terms linear and quadratic in the transverse momenta \vec{k}_\perp which are neglected in the Hamiltonian H_0 of collinear QCD. We can write the exact eigensolution of the full Hamiltonian as

$$\psi_{(3+1)} = \psi_{(1+1)} + \frac{1}{M^2 - H + i\epsilon} \Delta H \psi_{(1+1)} ,$$

where

$$\frac{1}{M^2 - H + i\epsilon} = \frac{1}{M^2 - H_0 + i\epsilon} + \frac{1}{M^2 - H + i\epsilon} \Delta H \frac{1}{M^2 - H_0 + i\epsilon}$$

can be represented as the continued iteration of the Lippmann Schwinger resolvent. Note that the matrix $(M^2 - H_0)^{-1}$ is known to any desired precision from the DLCQ solution of collinear QCD.

3 Electroweak Matrix Elements and Light-Cone Wavefunctions

Another remarkable advantage of the light-cone formalism is that exclusive semileptonic B -decay amplitudes such as $B \rightarrow A\ell\bar{\nu}$ can be evaluated exactly [35]. The timelike decay matrix elements require the computation of the diagonal matrix element $n \rightarrow n$ where parton number is conserved, and the off-diagonal $n + 1 \rightarrow n - 1$

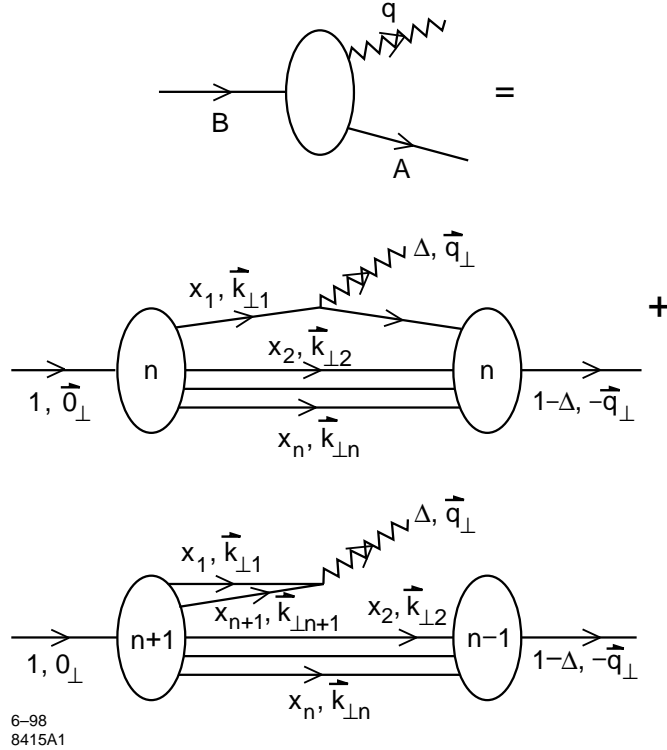


Figure 1: Exact representation of electroweak decays and time-like form factors in the light-cone Fock representation.

convolution where the current operator annihilates a $q\bar{q}$ pair in the initial B wavefunction. See Fig. 1. This term is a consequence of the fact that the time-like decay $q^2 = (p_\ell + p_{\bar{\nu}})^2 > 0$ requires a positive light-cone momentum fraction $q^+ > 0$. Conversely for space-like currents, one can choose $q^+ = 0$, as in the Drell-Yan-West representation of the space-like electromagnetic form factors. However, as can be seen from the explicit analysis of the form factor in a perturbative model, the off-diagonal convolution can yield a nonzero q^+/q^+ limiting form as $q^+ \rightarrow 0$. This extra term appears specifically in the case of “bad” currents such as J^- in which the coupling to $q\bar{q}$ fluctuations in the light-cone wavefunctions are favored. In effect, the $q^+ \rightarrow 0$ limit generates $\delta(x)$ contributions as residues of the $n+1 \rightarrow n-1$ contributions. The necessity for such “zero mode” $\delta(x)$ terms has been noted by Chang, Root and Yan [36], Burkardt [37], and Ji and Choi [38].

The off-diagonal $n+1 \rightarrow n-1$ contributions give a new perspective for the

physics of B -decays. A semileptonic decay involves not only matrix elements where a quark changes flavor, but also a contribution where the leptonic pair is created from the annihilation of a $q\bar{q}'$ pair within the Fock states of the initial B wavefunction. The semileptonic decay thus can occur from the annihilation of a nonvalence quark-antiquark pair in the initial hadron. This feature will carry over to exclusive hadronic B -decays, such as $B^0 \rightarrow \pi^- D^+$. In this case the pion can be produced from the coalescence of a $d\bar{u}$ pair emerging from the initial higher particle number Fock wavefunction of the B . The D meson is then formed from the remaining quarks after the internal exchange of a W boson.

In principle, a precise evaluation of the hadronic matrix elements needed for B -decays and other exclusive electroweak decay amplitudes requires knowledge of all of the light-cone Fock wavefunctions of the initial and final state hadrons. In the case of model gauge theories such as QCD(1+1) [39] or collinear QCD [19] in one-space and one-time dimensions, the complete evaluation of the light-cone wavefunction is possible for each baryon or meson bound-state using the DLCQ method. It would be interesting to use such solutions as a model for physical B -decays.

The existence of an exact formalism for electroweak matrix elements gives a basis for systematic approximations and a control over neglected terms. For example, one can analyze exclusive semileptonic B -decays which involve hard internal momentum transfer using a perturbative QCD formalism patterned after the analysis of form factors at large momentum transfer [11]. The hard-scattering analysis proceeds by writing each hadronic wavefunction as a sum of soft and hard contributions

$$\psi_n = \psi_n^{\text{soft}}(\mathcal{M}_n^2 < \Lambda^2) + \psi_n^{\text{hard}}(\mathcal{M}_n^2 > \Lambda^2), \quad (7)$$

where \mathcal{M}_n^2 is the invariant mass of the partons in the n -particle Fock state and Λ is the separation scale. The high internal momentum contributions to the wavefunction ψ_n^{hard} can be calculated systematically from QCD perturbation theory by iterating the gluon exchange kernel. The contributions from high momentum transfer exchange to the B -decay amplitude can then be written as a convolution of a hard scattering quark-gluon scattering amplitude T_H with the distribution amplitudes $\phi(x_i, \Lambda)$, the valence wavefunctions obtained by integrating the constituent momenta up to the separation scale $\mathcal{M}_n < \Lambda < Q$. This is the basis for the perturbative hard scattering analyses [13, 15, 40, 16]. In the exact analysis, one can identify the hard PQCD

contribution as well as the soft contribution from the convolution of the light-cone wavefunctions. Furthermore, the hard scattering contribution can be systematically improved. For example, off-shell effects can be retained in the evaluation of T_H by utilizing the exact light-cone energy denominators.

Given the solution for the hadronic wavefunctions $\psi_n^{(\Lambda)}$ with $\mathcal{M}_n^2 < \Lambda^2$, one can construct the wavefunction in the hard regime with $\mathcal{M}_n^2 > \Lambda^2$ using projection operator techniques [11]. The construction can be done perturbatively in QCD since only high invariant mass, far off-shell matrix elements are involved. One can use this method to derive the physical properties of the LC wavefunctions and their matrix elements at high invariant mass. Since $\mathcal{M}_n^2 = \sum_{i=1}^n \left(\frac{k_{\perp}^2 + m^2}{x} \right)_i$, this method also allows the derivation of the asymptotic behavior of light-cone wavefunctions at large k_{\perp} , which in turn leads to predictions for the fall-off of form factors and other exclusive matrix elements at large momentum transfer, such as the quark counting rules for predicting the nominal power-law fall-off of two-body scattering amplitudes at fixed θ_{cm} [41]. The phenomenological successes of these rules can be understood within QCD if the coupling $\alpha_V(Q)$ freezes in a range of relatively small momentum transfer [32].

4 Other Applications of Light-Cone Quantization to QCD Phenomenology

Diffractive vector meson photoproduction. The light-cone Fock wavefunction representation of hadronic amplitudes allows a simple eikonal analysis of diffractive high energy processes, such as $\gamma^*(Q^2)p \rightarrow \rho p$, in terms of the virtual photon and the vector meson Fock state light-cone wavefunctions convoluted with the $gp \rightarrow gp$ near-forward matrix element [42]. One can easily show that only small transverse size $b_{\perp} \sim 1/Q$ of the vector meson distribution amplitude is involved. The hadronic interactions are minimal, and thus the $\gamma^*(Q^2)N \rightarrow \rho N$ reaction can occur coherently throughout a nuclear target in reactions without absorption or shadowing. The $\gamma^*A \rightarrow VA$ process thus is a laboratory for testing QCD color transparency [9]. This is discussed further in the next section.

Regge behavior of structure functions. The light-cone wavefunctions $\psi_{n/H}$ of a

hadron are not independent of each other, but rather are coupled via the equations of motion. Antonuccio, Dalley and I [43] have used the constraint of finite “mechanical” kinetic energy to derive “ladder relations” which interrelate the light-cone wavefunctions of states differing by one or two gluons. We then use these relations to derive the Regge behavior of both the polarized and unpolarized structure functions at $x \rightarrow 0$, extending Mueller’s derivation of the BFKL hard QCD pomeron from the properties of heavy quarkonium light-cone wavefunctions at large N_C QCD [44].

Structure functions at large x_{bj} . The behavior of structure functions where one quark has the entire momentum requires the knowledge of LC wavefunctions with $x \rightarrow 1$ for the struck quark and $x \rightarrow 0$ for the spectators. This is a highly off-shell configuration, and thus one can rigorously derive quark-counting and helicity-retention rules for the power-law behavior of the polarized and unpolarized quark and gluon distributions in the $x \rightarrow 1$ endpoint domain. It is interesting to note that the evolution of structure functions is minimal in this domain because the struck quark is highly virtual as $x \rightarrow 1$; *i.e.* the starting point Q_0^2 for evolution cannot be held fixed, but must be larger than a scale of order $(m^2 + k_\perp^2)/(1 - x)$ [11, 41, 45].

Intrinsic gluon and heavy quarks. The main features of the heavy sea quark-pair contributions of the Fock state expansion of light hadrons can also be derived from perturbative QCD, since \mathcal{M}_n^2 grows with m_Q^2 . One identifies two contributions to the heavy quark sea, the “extrinsic” contributions which correspond to ordinary gluon splitting, and the “intrinsic” sea which is multi-connected via gluons to the valence quarks. The intrinsic sea is thus sensitive to the hadronic bound state structure [6]. The maximal contribution of the intrinsic heavy quark occurs at $x_Q \simeq m_\perp Q / \sum_i m_\perp$ where $m_\perp = \sqrt{m^2 + k_\perp^2}$; *i.e.* at large x_Q , since this minimizes the invariant mass \mathcal{M}_n^2 . The measurements of the charm structure function by the EMC experiment are consistent with intrinsic charm at large x in the nucleon with a probability of order $0.6 \pm 0.3\%$ [7]. Similarly, one can distinguish intrinsic gluons which are associated with multi-quark interactions and extrinsic gluon contributions associated with quark substructure [46]. One can also use this framework to isolate the physics of the anomaly contribution to the Ellis-Jaffe sum rule.

Materialization of far-off-shell configurations. In a high energy hadronic collisions, the highly-virtual states of a hadron can be materialized into physical hadrons simply by the soft interaction of any of the constituents [47]. Thus a proton state with

intrinsic charm $|uud\bar{c}c\rangle$ can be materialized, producing a J/ψ at large x_F , by the interaction of a light-quark in the target. The production occurs on the front-surface of a target nucleus, implying an $A^{2/3}$ J/ψ production cross section at large x_F , which is consistent with experiment, such as Fermilab experiments E772 and E866.

Rearrangement mechanism in heavy quarkonium decay. It is usually assumed that a heavy quarkonium state such as the J/ψ always decays to light hadrons via the annihilation of its heavy quark constituents to gluons. However, as Karliner and I [48] have recently shown, the transition $J/\psi \rightarrow \rho\pi$ can also occur by the rearrangement of the $c\bar{c}$ from the J/ψ into the $|q\bar{q}c\bar{c}\rangle$ intrinsic charm Fock state of the ρ or π . On the other hand, the overlap rearrangement integral in the decay $\psi' \rightarrow \rho\pi$ will be suppressed since the intrinsic charm Fock state radial wavefunction of the light hadrons will evidently not have nodes in its radial wavefunction. This observation gives a natural explanation of the long-standing puzzle why the J/ψ decays prominently to two-body pseudoscalar-vector final states, whereas the ψ' does not.

Asymmetry of intrinsic heavy quark sea. The higher Fock state of the proton $|uuds\bar{s}\rangle$ should resemble a $|K\Lambda\rangle$ intermediate state, since this minimizes its invariant mass \mathcal{M} . In such a state, the strange quark has a higher mean momentum fraction x than the \bar{s} [49, 50, 51]. Similarly, the helicity intrinsic strange quark in this configuration will be anti-aligned with the helicity of the nucleon [49, 51]. This $Q \leftrightarrow \bar{Q}$ asymmetry is a striking feature of the intrinsic heavy-quark sea.

Comover phenomena. Light-cone wavefunctions describe not only the partons that interact in a hard subprocess but also the associated partons freed from the projectile. The projectile partons which are comoving (*i.e.*, which have similar rapidity) with final state quarks and gluons can interact strongly producing (a) leading particle effects, such as those seen in open charm hadroproduction; (b) suppression of quarkonium [52] in favor of open heavy hadron production, as seen in the E772 experiment; (c) changes in color configurations and selection rules in quarkonium hadroproduction, as has been emphasized by Hoyer and Peigne [53]. All of these effects violate the usual ideas of factorization for inclusive reactions. Further, more than one parton from the projectile can enter the hard subprocess, producing dynamical higher twist contributions, as seen for example in Drell-Yan experiments [54, 55].

Jet hadronization in light-cone QCD. One of the goals of nonperturbative analysis

in QCD is to compute jet hadronization from first principles. The DLCQ solutions provide a possible method to accomplish this. By inverting the DLCQ solutions, we can write the “bare” quark state of the free theory as $|q_0\rangle = \sum |n\rangle \langle n|q_0\rangle$ where now $\{|n\rangle\}$ are the exact DLCQ eigenstates of H_{LC} , and $\langle n|q_0\rangle$ are the DLCQ projections of the eigensolutions. The expansion is automatically infrared and ultraviolet regulated if we impose global cutoffs on the DLCQ basis: $\lambda^2 < \Delta\mathcal{M}_n^2 < \Lambda^2$ where $\Delta\mathcal{M}_n^2 = \mathcal{M}_n^2 - (\sum\mathcal{M}_i)^2$. It would be interesting to study jet hadronization at the amplitude level for the existing DLCQ solutions to QCD (1+1) and collinear QCD.

Hidden Color. The deuteron form factor at high Q^2 is sensitive to wavefunction configurations where all six quarks overlap within an impact separation $b_{\perp i} < \mathcal{O}(1/Q)$; the leading power-law fall off predicted by QCD is $F_d(Q^2) = f(\alpha_s(Q^2))/(Q^2)^5$, where, asymptotically, $f(\alpha_s(Q^2)) \propto \alpha_s(Q^2)^{5+2\gamma}$ [56]. The derivation of the evolution equation for the deuteron distribution amplitude and its leading anomalous dimension γ is given in Ref. [57] In general, the six-quark wavefunction of a deuteron is a mixture of five different color-singlet states. The dominant color configuration at large distances corresponds to the usual proton-neutron bound state. However at small impact space separation, all five Fock color-singlet components eventually acquire equal weight, *i.e.*, the deuteron wavefunction evolves to 80% “hidden color.” The relatively large normalization of the deuteron form factor observed at large Q^2 points to sizable hidden color contributions [58].

Spin-Spin Correlations in Nucleon-Nucleon Scattering and the Charm Threshold. One of the most striking anomalies in elastic proton-proton scattering is the large spin correlation A_{NN} observed at large angles [59]. At $\sqrt{s} \simeq 5$ GeV, the rate for scattering with incident proton spins parallel and normal to the scattering plane is four times larger than that for scattering with anti-parallel polarization. This strong polarization correlation can be attributed to the onset of charm production in the intermediate state at this energy [60]. The intermediate state $|uud\bar{u}d\bar{c}\bar{c}\rangle$ has odd intrinsic parity and couples to the $J = S = 1$ initial state, thus strongly enhancing scattering when the incident projectile and target protons have their spins parallel and normal to the scattering plane. The charm threshold can also explain the anomalous change in color transparency observed at the same energy in quasi-elastic pp scattering. A crucial test is the observation of open charm production near threshold with a cross section of order of $1\mu\text{b}$.

5 Features of Hard Exclusive Processes in QCD

Exclusive and diffractive reactions are highly challenging to analyze in QCD since they require knowledge of the hadron wavefunctions at the amplitude level. There has been much progress analyzing exclusive and diffractive reactions at large momentum transfer from first principles in QCD. Rigorous statements can be made on the basis of asymptotic freedom and factorization theorems which separate the underlying hard quark and gluon subprocess amplitude from the nonperturbative physics incorporated into the process-independent hadron distribution amplitudes $\phi_H(x_i, Q)$ [11], the valence light-cone wavefunctions integrated over $k_\perp^2 < Q^2$.

In general, hard exclusive hadronic amplitudes such as quarkonium decay, heavy hadron decay, and scattering amplitudes where hadrons are scattered with large momentum transfer can be factorized at leading power as a convolution of distribution amplitudes and hard-scattering quark/gluon matrix elements [11]

$$\begin{aligned} \mathcal{M}_{\text{Hadron}} = & \prod_H \sum_n \int \prod_{i=1}^n d^2 k_\perp \prod_{i=1}^n dx \delta\left(1 - \sum_{i=1}^n x_i\right) \delta\left(\sum_{i=1}^n \vec{k}_{\perp i}\right) \\ & \times \psi_{n/H}^{(\lambda)}(x_i, \vec{k}_{\perp i}, \lambda_i) T_H^{(\Lambda)}. \end{aligned} \quad (8)$$

Here $T_H^{(\Lambda)}$ is the underlying quark-gluon subprocess scattering amplitude in which the (incident and final) hadrons are replaced by their respective quarks and gluons with momenta $x_i p^+$, $x_i \vec{p}_\perp + \vec{k}_{\perp i}$ and invariant mass above the separation scale $\mathcal{M}_n^2 > \Lambda^2$. At large Q^2 one can integrate over the transverse momenta. The leading power behavior of the hard quark-gluon scattering amplitude $T_H(\vec{k}_{\perp i} = 0)$, defined for the case where the quarks are effectively collinear with their respective parent hadron's momentum, provides the basic scaling and helicity features of the hadronic amplitude. The essential part of the hadron wavefunction is the hadronic distribution amplitudes [11], defined as the integral over transverse momenta of the valence (lowest particle number) Fock wavefunction, as defined in Eq. (5) where the global cutoff Λ is identified with the resolution Q . The distribution amplitude controls leading-twist exclusive amplitudes at high momentum transfer, and it can be related to the gauge-invariant Bethe-Salpeter wavefunction at equal light-cone time $\tau = x^+$.

The $\log Q$ evolution of the hadron distribution amplitudes $\phi_H(x_i, Q)$ can be derived from the perturbatively-computable tail of the valence light-cone wavefunction

in the high transverse momentum regime. The LC ultraviolet regulators provide a factorization scheme for elastic and inelastic scattering, separating the hard dynamical contributions with invariant mass squared $\mathcal{M}^2 > \Lambda_{\text{global}}^2$ from the soft physics with $\mathcal{M}^2 \leq \Lambda_{\text{global}}^2$ which is incorporated in the nonperturbative LC wavefunctions. The DGLAP evolution of quark and gluon distributions can also be derived in an analogous way by computing the variation of the Fock expansion with respect to Λ^2 . The renormalization scale ambiguities in hard-scattering amplitudes via commensurate scale relations [24, 25, 26] which connect the couplings entering exclusive amplitudes to the α_V coupling which controls the QCD heavy quark potential [61].

The features of exclusive processes to leading power in the transferred momenta are well known:

(1) The leading power fall-off is given by dimensional counting rules for the hard-scattering amplitude: $T_H \sim 1/Q^{n-1}$, where n is the total number of fields (quarks, leptons, or gauge fields) participating in the hard scattering [62, 63]. Thus the reaction is dominated by subprocesses and Fock states involving the minimum number of interacting fields. The hadronic amplitude follows this fall-off modulo logarithmic corrections from the running of the QCD coupling, and the evolution of the hadron distribution amplitudes. In some cases, such as large angle $pp \rightarrow pp$ scattering, pinch contributions from multiple hard-scattering processes must also be included [64]. The general success of dimensional counting rules implies that the effective coupling $\alpha_V(Q^*)$ controlling the gluon exchange propagators in T_H are frozen in the infrared, *i.e.*, have an infrared fixed point, since the effective momentum transfers Q^* exchanged by the gluons are often a small fraction of the overall momentum transfer [61]. The pinch contributions are then suppressed by a factor decreasing faster than a fixed power [62].

(2) The leading power dependence is given by hard-scattering amplitudes T_H which conserve quark helicity [65, 66]. Since the convolution of T_H with the light-cone wavefunctions projects out states with $L_z = 0$, the leading hadron amplitudes conserve hadron helicity; *i.e.*, the sum of initial and final hadron helicities are conserved. Hadron helicity conservation thus follows from the underlying chiral structure of QCD.

(3) Since the convolution of the hard scattering amplitude T_H with the light-cone wavefunctions projects out the valence states with small impact parameter, the essen-

tial part of the hadron wavefunction entering a hard exclusive amplitude has a small color dipole moment. This leads to the absence of initial or final state interactions among the scattering hadrons as well as the color transparency of quasi-elastic interactions in a nuclear target [9, 67]. Color transparency reflects the underlying gauge theoretic basis of the strong interactions. For example, the amplitude for diffractive vector meson photoproduction $\gamma^*(Q^2)p \rightarrow \rho p$, can be written as convolution of the virtual photon and the vector meson Fock state light-cone wavefunctions the $gp \rightarrow gp$ near-forward matrix element [42]. One can easily show that only small transverse size $b_\perp \sim 1/Q$ of the vector meson distribution amplitude is involved. The sum over the interactions of the exchanged gluons tend to cancel reflecting its small color dipole moment. Since the hadronic interactions are minimal, the $\gamma^*(Q^2)N \rightarrow \rho N$ reaction at large Q^2 can occur coherently throughout a nuclear target in reactions without absorption or final state interactions. The $\gamma^*A \rightarrow VA$ process thus provides a natural framework for testing QCD color transparency. Evidence for color transparency in such reactions has been found by Fermilab experiment E665 [68].

(4) The evolution equations for distribution amplitudes which incorporate the operator product expansion, renormalization group invariance, and conformal symmetry [11, 22, 23, 69, 70].

(5) Hidden color degrees of freedom in nuclear wavefunctions reflects the complex color structure of hadron and nuclear wavefunctions [57]. The hidden color increases the normalization of nuclear amplitudes such as the deuteron form factor at large momentum transfer.

The field of analyzable exclusive processes has recently been expanded to a new range of QCD processes, such as the highly virtual diffractive processes $\gamma^*p \rightarrow \rho p$ [42, 71], and semi-exclusive processes such as $\gamma^*p \rightarrow \pi^+ X$ [72, 73, 74] where the π^+ is produced in isolation at large p_T . An important new application of the perturbative QCD analysis of exclusive processes is the recent analysis of hard B decays such as $B \rightarrow \pi\pi$ by Beneke, *et al.* [14]

Exclusive hard-scattering reactions and hard diffractive reactions are now giving a valuable window into the structure and dynamics of hadronic amplitudes. Recent measurements of the photon-to-pion transition form factor at CLEO [75], the diffractive dissociation of pions into jets at Fermilab [76], diffractive vector meson leptonproduction at Fermilab and HERA, and the new program of experiments on exclusive

proton and deuteron processes at Jefferson Laboratory are now yielding fundamental information on hadronic wavefunctions, particularly the distribution amplitude of mesons. Such information is also critical for interpreting exclusive heavy hadron decays and the matrix elements and amplitudes entering CP -violating processes at the B factories.

There has been much progress analyzing exclusive and diffractive reactions at large momentum transfer from first principles in QCD. Rigorous statements can be made on the basis of asymptotic freedom and factorization theorems which separate the underlying hard quark and gluon subprocess amplitude from the nonperturbative physics incorporated into the process-independent hadron distribution amplitudes $\phi_H(x_i, Q)$ [11]. An important new application is the recent analysis of hard exclusive B decays by Beneke, *et al.* [14] Key features of such analyses are: (a) evolution equations for distribution amplitudes which incorporate the operator product expansion, renormalization group invariance, and conformal symmetry [11, 22, 77, 23, 69, 70]; (b) hadron helicity conservation which follows from the underlying chiral structure of QCD [65]; (c) color transparency, which eliminates corrections to hard exclusive amplitudes from initial and final state interactions at leading power and reflects the underlying gauge theoretic basis for the strong interactions [9, 67]; and (d) hidden color degrees of freedom in nuclear wavefunctions, which reflects the color structure of hadron and nuclear wavefunctions [57]. There have also been recent advances eliminating renormalization scale ambiguities in hard-scattering amplitudes via commensurate scale relations [24, 25, 26] which connect the couplings entering exclusive amplitudes to the α_V coupling which controls the QCD heavy quark potential [61]. The postulate that the QCD coupling has an infrared fixed-point can explain the applicability of conformal scaling and dimensional counting rules to physical QCD processes [62, 63, 61]. The field of analyzable exclusive processes has recently been expanded to a new range of QCD processes, such as electroweak decay amplitudes, highly virtual diffractive processes such as $\gamma^*p \rightarrow \rho p$ [42, 78], and semi-exclusive processes such as $\gamma^*p \rightarrow \pi^+ X$ [72, 73, 74] where the π^+ is produced in isolation at large p_T .

The natural renormalization scheme for the QCD coupling in hard exclusive processes is $\alpha_V(Q)$, the effective charge defined from the scattering of two infinitely-heavy quark test charges. The renormalization scale can then be determined from the vir-

tuality of the exchanged momentum of the gluons, as in the BLM and commensurate scale methods [31, 24, 25, 26]. We will discuss these theoretical tools and methods in the later sections.

The main features of exclusive processes to leading power in the transferred momenta are:

(1) The leading power fall-off is given by dimensional counting rules for the hard-scattering amplitude: $T_H \sim 1/Q^{n-1}$, where n is the total number of fields (quarks, leptons, or gauge fields) participating in the hard scattering [62, 63]. Thus the reaction is dominated by subprocesses and Fock states involving the minimum number of interacting fields. The hadronic amplitude follows this fall-off modulo logarithmic corrections from the running of the QCD coupling, and the evolution of the hadron distribution amplitudes. In some cases, such as large angle $pp \rightarrow pp$ scattering, pinch contributions from multiple hard-scattering processes must also be included [64]. The general success of dimensional counting rules implies that the effective coupling $\alpha_V(Q^*)$ controlling the gluon exchange propagators in T_H are frozen in the infrared, *i.e.*, have an infrared fixed point, since the effective momentum transfers Q^* exchanged by the gluons are often a small fraction of the overall momentum transfer [61]. The pinch contributions are suppressed by a factor decreasing faster than a fixed power [62].

(2) The leading power dependence is given by hard-scattering amplitudes T_H which conserve quark helicity [65, 66]. Since the convolution of T_H with the light-cone wavefunctions projects out states with $L_z = 0$, the leading hadron amplitudes conserve hadron helicity; *i.e.*, the sum of initial and final hadron helicities are conserved.

(3) Since the convolution of the hard scattering amplitude T_H with the light-cone wavefunctions projects out the valence states with small impact parameter, the essential part of the hadron wavefunction entering a hard exclusive amplitude has a small color dipole moment. This leads to the absence of initial or final state interactions among the scattering hadrons as well as the color transparency. of quasi-elastic interactions in a nuclear target [9, 67]. For example, the amplitude for diffractive vector meson photoproduction $\gamma^*(Q^2)p \rightarrow \rho p$, can be written as convolution of the virtual photon and the vector meson Fock state light-cone wavefunctions the $gp \rightarrow gp$ near-forward matrix element [42]. One can easily show that only small transverse size

$b_{\perp} \sim 1/Q$ of the vector meson distribution amplitude is involved. The sum over the interactions of the exchanged gluons tend to cancel reflecting its small color dipole moment. Since the hadronic interactions are minimal, the $\gamma^*(Q^2)N \rightarrow \rho N$ reaction at large Q^2 can occur coherently throughout a nuclear target in reactions without absorption or final state interactions. The $\gamma^*A \rightarrow VA$ process thus provides a natural framework for testing QCD color transparency. Evidence for color transparency in such reactions has been found by Fermilab experiment E665 [68].

Diffraction multi-jet production in heavy nuclei provides a novel way to measure the shape of the LC Fock state wavefunctions and test color transparency. For example, consider the reaction [79, 80, 81] $\pi A \rightarrow \text{Jet}_1 + \text{Jet}_2 + A'$ at high energy where the nucleus A' is left intact in its ground state. The transverse momenta of the jets have to balance so that $\vec{k}_{\perp 1} + \vec{k}_{\perp 2} = \vec{q}_{\perp} < R^{-1}_A$, and the light-cone longitudinal momentum fractions have to add to $x_1 + x_2 \sim 1$ so that $\Delta p_L < R_A^{-1}$. The process can then occur coherently in the nucleus. Because of color transparency, *i.e.*, the cancelation of color interactions in a small-size color-singlet hadron, the valence wavefunction of the pion with small impact separation will penetrate the nucleus with minimal interactions, diffracting into jet pairs [79]. The $x_1 = x, x_2 = 1 - x$ dependence of the di-jet distributions will thus reflect the shape of the pion distribution amplitude; the $\vec{k}_{\perp 1} - \vec{k}_{\perp 2}$ relative transverse momenta of the jets also gives key information on the underlying shape of the valence pion wavefunction [80, 81]. The QCD analysis can be confirmed by the observation that the diffractive nuclear amplitude extrapolated to $t = 0$ is linear in nuclear number A , as predicted by QCD color transparency. The integrated diffractive rate should scale as $A^2/R_A^2 \sim A^{4/3}$. A diffractive dissociation experiment of this type, E791, is now in progress at Fermilab using 500 GeV incident pions on nuclear targets [76]. The preliminary results from E791 appear to be consistent with color transparency. The momentum fraction distribution of the jets is consistent with a valence light-cone wavefunction of the pion consistent with the shape of the asymptotic distribution amplitude, $\phi_{\pi}^{\text{asympt}}(x) = \sqrt{3}f_{\pi}x(1-x)$. As discussed below, data from CLEO [75] for the $\gamma\gamma^* \rightarrow \pi^0$ transition form factor also favor a form for the pion distribution amplitude close to the asymptotic solution [11] to the perturbative QCD evolution equation [82, 83, 61, 84, 85]. It will also be interesting to study diffractive tri-jet production using proton beams $pA \rightarrow \text{Jet}_1 + \text{Jet}_2 + \text{Jet}_3 + A'$ to determine the fundamental shape of the 3-quark structure of the valence light-cone wavefunction

of the nucleon at small transverse separation [80]. One interesting possibility is that the distribution amplitude of the $\Delta(1232)$ for $J_z = 1/2, 3/2$ is close to the asymptotic form $x_1 x_2 x_3$, but that the proton distribution amplitude is more complex. This would explain why the $p \rightarrow \Delta$ transition form factor appears to fall faster at large Q^2 than the elastic $p \rightarrow p$ and the other $p \rightarrow N^*$ transition form factors [86]. Conversely, one can use incident real and virtual photons: $\gamma^* A \rightarrow \text{Jet}_1 + \text{Jet}_2 + A'$ to confirm the shape of the calculable light-cone wavefunction for transversely-polarized and longitudinally-polarized virtual photons. Such experiments will open up a direct window on the amplitude structure of hadrons at short distances.

There are a large number of measured exclusive reactions in which the empirical power law fall-off predicted by dimensional counting and PQCD appears to be accurate over a large range of momentum transfer. These include processes such as the proton form factor, time-like meson pair production in e^+e^- and $\gamma\gamma$ annihilation, large-angle scattering processes such as pion photoproduction $\gamma p \rightarrow \pi^+ p$, and nuclear processes such as the deuteron form factor at large momentum transfer and deuteron photodisintegration [56]. A spectacular example is the recent measurements at CESR of the photon to pion transition form factor in the reaction $e\gamma \rightarrow e\pi^0$ [75]. As predicted by leading twist QCD [11] $Q^2 F_{\gamma\pi^0}(Q^2)$ is essentially constant for $1 \text{ GeV}^2 < Q^2 < 10 \text{ GeV}^2$. Further, the normalization is consistent with QCD at NLO if one assumes that the pion distribution amplitude takes on the form $\phi_\pi^{\text{asympt}}(x) = \sqrt{3} f_\pi x(1-x)$ which is the asymptotic solution [11] to the evolution equation for the pion distribution amplitude [82, 83, 61, 85].

If the pion distribution amplitude is close to its asymptotic form, then one can predict the normalization of exclusive amplitudes such as the spacelike pion form factor $Q^2 F_\pi(Q^2)$. Next-to-leading order predictions are now becoming available which incorporate higher order corrections to the pion distribution amplitude as well as the hard scattering amplitude [23, 87, 88]. However, the normalization of the PQCD prediction for the pion form factor depends directly on the value of the effective coupling $\alpha_V(Q^*)$ at momenta $Q^{*2} \simeq Q^2/20$. Assuming $\alpha_V(Q^*) \simeq 0.4$, the QCD LO prediction appears to be smaller by approximately a factor of 2 compared to the presently available data extracted from the original pion electroproduction experiments from CEA [89]. A definitive comparison will require a careful extrapolation to the pion pole and extraction of the longitudinally polarized photon contribution of the $ep \rightarrow \pi^+ n$ data.

The measured deuteron form factor and the deuteron photodisintegration cross section appear to follow the leading-twist QCD predictions at large momentum transfers in the few GeV region [90, 91]. The normalization of the measured deuteron form factor is large compared to model calculations [58] assuming that the deuteron's six-quark wavefunction can be represented at short distances with the color structure of two color singlet baryons. This provides indirect evidence for the presence of hidden color components as required by PQCD [57].

There are, however, experimental exceptions to the general success of the leading twist PQCD approach, such as (a) the dominance of the $J/\psi \rightarrow \rho\pi$ decay which is forbidden by hadron helicity conservation and (b) the strong normal-normal spin asymmetry A_{NN} observed in polarized elastic $pp \rightarrow pp$ scattering and an apparent breakdown of color transparency at large CM angles and $E_{CM} \sim 5$ GeV. These conflicts with leading-twist PQCD predictions can be used to identify the presence of new physical effects. For example, It is usually assumed that a heavy quarkonium state such as the J/ψ always decays to light hadrons via the annihilation of its heavy quark constituents to gluons. However, the transition $J/\psi \rightarrow \rho\pi$ can also occur by the rearrangement of the $c\bar{c}$ from the J/ψ into the $|q\bar{q}c\bar{c}\rangle$ intrinsic charm Fock state of the ρ or π [48]. On the other hand, the overlap rearrangement integral in the decay $\psi' \rightarrow \rho\pi$ will be suppressed since the intrinsic charm Fock state radial wavefunction of the light hadrons will evidently not have nodes in its radial wavefunction. This observation provides a natural explanation of the long-standing puzzle why the J/ψ decays prominently to two-body pseudoscalar-vector final states, whereas the ψ' does not. The unusual effects seen in elastic proton-proton scattering at $E_{CM} \sim 5$ GeV and large angles could be related to the charm threshold and the effect of a $|uud\bar{u}d\bar{c}\bar{c}\rangle$ resonance which would appear as in the $J = L = S = 1$ pp partial wave [60].

Recent experiments at Jefferson laboratory utilizing a new polarization transfer technique indicate that $G_E(Q^2)/G_M(Q^2)$ falls with increasing momentum transfer $-t = Q^2$ in the measured domain $1 < Q^2 < 3$ GeV² [92]. This observation implies that the helicity-changing Pauli form factor $F_2(Q^2)$ is comparable to the helicity conserving form factor $F_1(Q^2)$ in this domain. If such a trend continues to larger Q^2 it would be in severe conflict with the hadron-helicity conserving principle of perturbative QCD. If F_2 were comparable to F_1 at large Q^2 in the case of timelike processes, such as $p\bar{p} \rightarrow e^+e^-$, where $G_E = F_1 + \frac{Q^2}{4M_N^2}F_2$, one would see strong deviations from the usual

$1 + \cos^2 \theta$ dependence of the differential cross section as well as PQCD scaling. This seems to be in conflict with the available data from the $E835 \bar{p}p \rightarrow e^+e^-$ experiment at Fermilab [93].

A debate has continued on whether processes such as the pion and proton form factors and elastic Compton scattering $\gamma p \rightarrow \gamma p$ might be dominated by higher twist mechanisms until very large momentum transfers [94, 95, 96]. For example, if one assumes that the light-cone wavefunction of the pion has the form $\psi_{\text{soft}}(x, k_{\perp}) = A \exp(-b \frac{k_{\perp}^2}{x(1-x)})$, then the Feynman endpoint contribution to the overlap integral at small k_{\perp} and $x \simeq 1$ will dominate the form factor compared to the hard-scattering contribution until very large Q^2 . However, the above form of $\psi_{\text{soft}}(x, k_{\perp})$ has no suppression at $k_{\perp} = 0$ for any x ; *i.e.*, the wavefunction in the hadron rest frame does not fall-off at all for $k_{\perp} = 0$ and $k_z \rightarrow -\infty$. Thus such wavefunctions do not represent soft QCD contributions. Furthermore, such endpoint contributions will be suppressed by the QCD Sudakov form factor, reflecting the fact that a near-on-shell quark must radiate if it absorbs large momentum. If the endpoint contribution dominates proton Compton scattering, then both photons will interact on the same quark line in a local fashion, and the amplitude is predicted to be real, in strong contrast to the complex phase structure of the PQCD predictions. It should be noted that there is no apparent endpoint contribution which could explain the success of dimensional counting (s^{-7} scaling at fixed θ_{cm}) in large-angle pion photoproduction.

The perturbative QCD predictions [97] for the Compton amplitude phase can be tested in virtual Compton scattering by interference with Bethe-Heitler processes [98]. One can also measure the interference of deeply virtual Compton amplitudes with the timelike form factors by studying reactions in e^+e^- colliders such as $e^+e^- \rightarrow \pi^+\pi^-\gamma$. The asymmetry with respect to the electron or positron beam measures the interference of the Compton diagrams with the amplitude in which the photon is emitted from the lepton line.

It is interesting to compare the corresponding calculations of form factors of bound states in QED. The soft wavefunction is the Schrödinger-Coulomb solution $\psi_{1s}(\vec{k}) \propto (1 + \vec{p}^2/(\alpha m_{\text{red}})^2)^{-2}$, and the full wavefunction, which incorporates transversely polarized photon exchange, only differs by a factor $(1 + \vec{p}^2/m_{\text{red}}^2)$. Thus the leading twist dominance of form factors in QED occurs at relativistic scales $Q^2 > m_{\text{red}}^2$ [99]. Furthermore, there are no extra relative factors of α in the hard-scattering con-

tribution. If the QCD coupling α_V has an infrared fixed-point, then the fall-off of the valence wavefunctions of hadrons will have analogous power-law forms, consistent with the Abelian correspondence principle [28]. If such power-law wavefunctions are indeed applicable to the soft domain of QCD then, the transition to leading-twist power law behavior will occur in the nominal hard perturbative QCD domain where $Q^2 \gg \langle k_\perp^2 \rangle, m_q^2$.

6 Measurement of Light-cone Wavefunctions and Tests of Color Transparency via Diffractive Dissociation.

Diffractive multi-jet production in heavy nuclei provides a novel way to measure the shape of the LC Fock state wavefunctions and test color transparency. For example, consider the reaction [79, 80, 81] $\pi A \rightarrow \text{Jet}_1 + \text{Jet}_2 + A'$ at high energy where the nucleus A' is left intact in its ground state. The transverse momenta of the jets have to balance so that $\vec{k}_{\perp 1} + \vec{k}_{\perp 2} = \vec{q}_\perp < R^{-1}_A$, and the light-cone longitudinal momentum fractions have to add to $x_1 + x_2 \sim 1$ so that $\Delta p_L < R_A^{-1}$. The process can then occur coherently in the nucleus. Because of color transparency, *i.e.*, the cancelation of color interactions in a small-size color-singlet hadron, the valence wavefunction of the pion with small impact separation will penetrate the nucleus with minimal interactions, diffracting into jet pairs [79]. The two-gluon exchange process in effect differentiates the transverse momentum dependence of the hadron's wavefunction twice. Thus the $x_1 = x, x_2 = 1 - x$ dependence of the di-jet distributions will reflect the shape of the pion distribution amplitude; the $\vec{k}_{\perp 1} - \vec{k}_{\perp 2}$ relative transverse momenta of the jets also gives key information on the underlying shape of the valence pion wavefunction [80, 81]. The QCD analysis can be confirmed by the observation that the diffractive nuclear amplitude extrapolated to $t = 0$ is linear in nuclear number A , as predicted by QCD color transparency. The integrated diffractive rate should scale as $A^2/R_A^2 \sim A^{4/3}$. A diffractive dissociation experiment of this type, E791, is now in progress at Fermilab using 500 GeV incident pions on nuclear targets [76]. The preliminary results from E791 appear to be consistent with color transparency. The momentum fraction distribution of the jets is consistent with a valence light-cone wavefunction of the

pion consistent with the shape of the asymptotic distribution amplitude, $\phi_\pi^{\text{asympt}}(x) = \sqrt{3}f_\pi x(1-x)$. Data from CLEO [75] for the $\gamma\gamma^* \rightarrow \pi^0$ transition form factor also favor a form for the pion distribution amplitude close to the asymptotic solution [11] to the perturbative QCD evolution equation [82, 83, 61, 84, 85]. It is also possible that the distribution amplitude of the $\Delta(1232)$ for $J_z = 1/2, 3/2$ is close to the asymptotic form $x_1x_2x_3$, but that the proton distribution amplitude is more complex. This would explain why the $p \rightarrow \Delta$ transition form factor appears to fall faster at large Q^2 than the elastic $p \rightarrow p$ and the other $p \rightarrow N^*$ transition form factors [86]. It will thus be very interesting to study diffractive tri-jet production using proton beams dissociating into three jets on a nuclear target. $pA \rightarrow \text{Jet}_1 + \text{Jet}_2 + \text{Jet}_3 + A'$ to determine the fundamental shape of the 3-quark structure of the valence light-cone wavefunction of the nucleon at small transverse separation [80].

It is also interesting to consider the Coulomb dissociation of hadrons as a means to resolve their light-cone wavefunctions [100]. In the case of photon exchange, the transverse momentum dependence of the light-cone wavefunction is differentiated only once. For example, consider the process $ep \rightarrow e'\text{Jet}_1 + \text{Jet}_2 + \text{Jet}_3$ in which the proton dissociates into three distinct jets at large transverse momentum by scattering on an electron. In the case of an ep collider such as HERA, one can require all of the hadrons to be produced outside a forward annular exclusion zone, $\theta_H > \theta_{\text{min}}$, thus ensuring a minimum transverse momentum of each produced final state particle. The distribution of hadron longitudinal momentum in each azimuthal sector can be used to determine the underlying x_1, x_2, x_3 dependence of the proton's valence three-quark wavefunction. Such a procedure will allow the proton to self-resolve its fundamental structure. Similarly at lower momentum scales, one can study the dissociation of light nuclei into their nucleon and mesonic components in diffractive high momentum reactions.

One can use incident real and virtual photons: $\gamma^*A \rightarrow \text{Jet}_1 + \text{Jet}_2 + A'$ to confirm the shape of the calculable light-cone wavefunction for transversely-polarized and longitudinally-polarized virtual photons. At low transverse momentum, one expects interesting nonperturbative modifications. Such experiments will open up a direct window on the amplitude structure of hadrons at short distances.

7 Semi-Exclusive Processes: New Probes of Hadron Structure

A new class of hard “semi-exclusive” processes of the form $A + B \rightarrow C + Y$, have been proposed as new probes of QCD [74, 72, 73]. These processes are characterized by a large momentum transfer $t = (p_A - p_C)^2$ and a large rapidity gap between the final state particle C and the inclusive system Y . Here A, B and C can be hadrons or (real or virtual) photons. The cross sections for such processes factorize in terms of the distribution amplitudes of A and C and the parton distributions in the target B . Because of this factorization semi-exclusive reactions provide a novel array of generalized currents, which not only give insight into the dynamics of hard scattering QCD processes, but also allow experimental access to new combinations of the universal quark and gluon distributions.

QCD scattering amplitude for deeply virtual exclusive processes like Compton scattering $\gamma^*p \rightarrow \gamma p$ and meson production $\gamma^*p \rightarrow Mp$ factorizes into a hard subprocess and soft universal hadronic matrix elements [101, 78, 42]. For example, consider exclusive meson electroproduction such as $ep \rightarrow e\pi^+n$ (Fig. 2a). Here one takes (as in DIS) the Bjorken limit of large photon virtuality, with $x_B = Q^2/(2m_p\nu)$ fixed, while the momentum transfer $t = (p_p - p_n)^2$ remains small. These processes involve ‘skewed’ parton distributions, which are generalizations of the usual parton distributions measured in DIS. The skewed distribution in Fig. 2a describes the emission of a u -quark from the proton target together with the formation of the final neutron from the d -quark and the proton remnants. As the subenergy \hat{s} of the scattering process $\gamma^*u \rightarrow \pi^+d$ is not fixed, the amplitude involves an integral over the u -quark momentum fraction x .

An essential condition for the factorization of the deeply virtual meson production amplitude of Fig. 2a is the existence of a large rapidity gap between the produced meson and the neutron. This factorization remains valid if the neutron is replaced with a hadronic system Y of invariant mass $M_Y^2 \ll W^2$, where W is the c.m. energy of the γ^*p process. For $M_Y^2 \gg m_p^2$ the momentum k' of the d -quark in Fig. 2b is large with respect to the proton remnants, and hence it forms a jet. This jet hadronizes independently of the other particles in the final state if it is not in the direction of the meson, *i.e.*, if the meson has a large transverse momentum $q'_\perp = \Delta_\perp$ with respect to

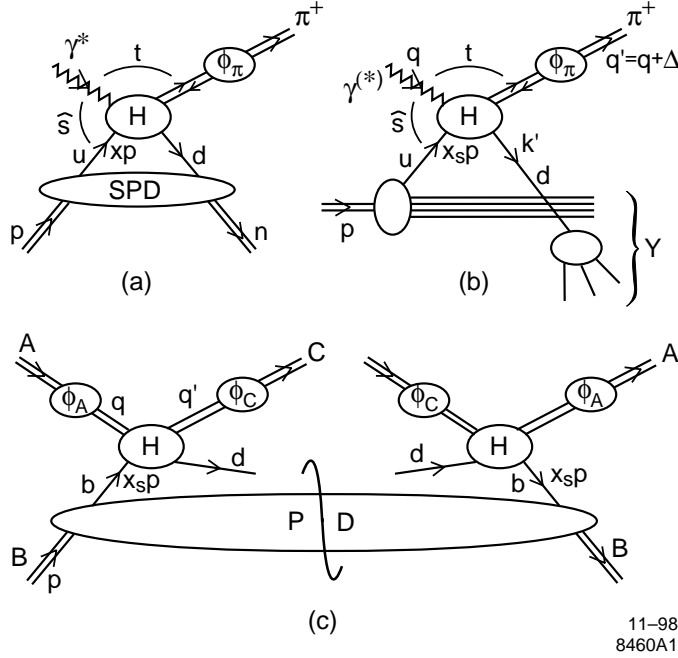


Figure 2: (a): Factorization of $\gamma^*p \rightarrow \pi^+n$ into a skewed parton distribution (SPD), a hard scattering H and the pion distribution amplitude ϕ_π . (b): Semi-exclusive process $\gamma^{(*)}p \rightarrow \pi^+Y$. The d -quark produced in the hard scattering H hadronizes independently of the spectator partons in the proton. (c): Diagram for the cross section of a generic semi-exclusive process. It involves a hard scattering H , distribution amplitudes ϕ_A and ϕ_C and a parton distribution (PD) in the target B .

the photon direction in the γ^*p c.m. Then the cross section for an inclusive system Y can be calculated as in DIS, by treating the d -quark as a final state particle.

The large Δ_\perp furthermore allows only transversally compact configurations of the projectile A to couple to the hard subprocess H of Fig. 2b, as it does in exclusive processes [11]. Hence the above discussion applies not only to incoming virtual photons at large Q^2 , but also to real photons ($Q^2 = 0$) and in fact to any hadron projectile.

Let us then consider the general process $A + B \rightarrow C + Y$, where B and C are hadrons or real photons, while the projectile A can also be a virtual photon. In the semi-exclusive kinematic limit $\Lambda_{QCD}^2, M_B^2, M_C^2 \ll M_Y^2, \Delta_\perp^2 \ll W^2$ we have a large rapidity gap $|y_C - y_d| = \log \frac{W^2}{\Delta_\perp^2 + M_Y^2}$ between C and the parton d produced in the hard

scattering (see Fig. 2c). The cross section then factorizes into the form

$$\begin{aligned} \frac{d\sigma}{dt dx_S}(A + B \rightarrow C + Y) \\ = \sum_b f_{b/B}(x_S, \mu^2) \frac{d\sigma}{dt}(Ab \rightarrow Cd), \end{aligned} \quad (9)$$

where $t = (q - q')^2$ and $f_{b/B}(x_S, \mu^2)$ denotes the distribution of quarks, antiquarks and gluons b in the target B . The momentum fraction x_S of the struck parton b is fixed by kinematics to the value $x_S = \frac{-t}{M_Y^2 - t}$ and the factorization scale μ^2 is characteristic of the hard subprocess $Ab \rightarrow Cd$.

It is conceptually helpful to regard the hard scattering amplitude H in Fig. 2c as a generalized current of momentum $q - q' = p_A - p_C$, which interacts with the target parton b . For $A = \gamma^*$ we obtain a close analogy to standard DIS when particle C is removed. With $q' \rightarrow 0$ we thus find $-t \rightarrow Q^2$, $M_Y^2 \rightarrow W^2$, and see that x_S goes over into $x_B = Q^2/(W^2 + Q^2)$. The possibility to control the value of q' (and hence the momentum fraction x_S of the struck parton) as well as the quantum numbers of particles A and C should make semi-exclusive processes a versatile tool for studying hadron structure. The cross section further depends on the distribution amplitudes ϕ_A, ϕ_C (*c.f.* Fig. 2c), allowing new ways of measuring these quantities.

8 Conformal Symmetry as a Template

Testing quantum chromodynamics to high precision is not easy. Even in processes involving high momentum transfer, perturbative QCD predictions are complicated by questions of the convergence of the series, particularly by the presence of “renormalon” terms which grow as $n!$, reflecting the uncertainty in the analytic form of the QCD coupling at low scales. Virtually all QCD processes are complicated by the presence of dynamical higher twist effects, including power-law suppressed contributions due to multi-parton correlations, intrinsic transverse momentum, and finite quark masses. Many of these effects are inherently nonperturbative in nature and require knowledge of hadron wavefunction themselves. The problem of interpreting perturbative QCD predictions is further compounded by theoretical ambiguities due to the apparent freedom in the choice of renormalization schemes, renormalization scales, and factorization procedures.

A central principle of renormalization theory is that predictions which relate physical observables to each other cannot depend on theoretical conventions. For example, one can use any renormalization scheme, such as the modified minimal subtraction dimensional regularization scheme, and any choice of renormalization scale μ to compute perturbative series observables A and B . However, all traces of the choices of the renormalization scheme and scale must disappear when we algebraically eliminate the $\alpha_{\overline{MS}}(\mu)$ and directly relate A to B . This is the principle underlying “commensurate scale relations” (CSR) [24], which are general leading-twist QCD predictions relating physical observables to each other. For example, the “generalized Crewther relation”, which is discussed in more detail below, provides a scheme-independent relation between the QCD corrections to the Bjorken (or Gross Llewellyn-Smith) sum rule for deep inelastic lepton-nucleon scattering, at a given momentum transfer Q , to the radiative corrections to the annihilation cross section $\sigma_{e^+e^- \rightarrow \text{hadrons}}(s)$, at a corresponding “commensurate” energy scale \sqrt{s} [24, 25]. The specific relation between the physical scales Q and \sqrt{s} reflects the fact that the radiative corrections to each process have distinct quark mass thresholds.

Any perturbatively calculable physical quantity can be used to define an effective charge [102, 103, 104] by incorporating the entire radiative correction into its definition. For example, the $e^+e^- \gamma^* \rightarrow \text{hadrons}$ annihilation to muon pair cross section ratio can be written

$$R_{e^+e^-}(s) \equiv R_{e^+e^-}^0(s) \left[1 + \frac{\alpha_R(s)}{\pi} \right], \quad (10)$$

where $R_{e^+e^-}^0$ is the prediction at Born level. Similarly, we can define the entire radiative correction to the Bjorken sum rule as the effective charge $\alpha_{g_1}(Q^2)$ where Q is the corresponding momentum transfer:

$$\begin{aligned} \int_0^1 dx \left[g_1^{ep}(x, Q^2) - g_1^{en}(x, Q^2) \right] &\equiv \frac{1}{6} \left| \frac{g_A}{g_V} \right| C_{\text{Bj}}(Q^2) \\ &= \frac{1}{6} \left| \frac{g_A}{g_V} \right| \left[1 - \frac{3}{4} C_F \frac{\alpha_{g_1}(Q^2)}{\pi} \right]. \end{aligned} \quad (11)$$

By convention, each effective charge is normalized to α_s in the weak coupling limit. One can define effective charges for virtually any quantity calculable in perturbative QCD; *e.g.* moments of structure functions, ratios of form factors, jet observables, and the effective potential between massive quarks. In the case of decay constants of the Z or the τ , the mass of the decaying system serves as the physical scale in the effective

charge. In the case of multi-scale observables, such as the two-jet fraction in e^+e^- annihilation, the multiple arguments of the effective coupling $\alpha_{2jet}(s, y)$ correspond to the overall available energy s variables such as $y = \max_{ij}(p_i + p_j)^2/s$ representing the maximum jet mass fraction.

Commensurate scale relations take the general form

$$\alpha_A(Q_A) = C_{AB}[\alpha_B(Q_B)] . \quad (12)$$

The function $C_{AB}(\alpha_B)$ relates the observables A and B in the conformal limit; *i.e.*, C_{AB} gives the functional dependence between the effective charges which would be obtained if the theory had zero β function. The conformal coefficients can be distinguished from the terms associated with the β function at each order in perturbation theory from their color and flavor dependence, or by an expansion about a fixed point.

The ratio of commensurate scales is determined by the requirement that all terms involving the β function are incorporated into the arguments of the running couplings, as in the original BLM procedure. Physically, the ratio of scales corresponds to the fact that the physical observables have different quark threshold and distinct sensitivities to fermion loops. More generally, the differing scales are in effect relations between mean values of the physical scales which appear in loop integrations. Commensurate scale relations are transitive; *i.e.*, given the relation between effective charges for observables A and C and C and B , the resulting between A and B is independent of C . In particular, transitivity implies $\Lambda_{AB} = \Lambda_{AC} \times \Lambda_{CB}$.

One can consider QCD predictions as functions of analytic variables of the number of colors N_C and flavors N_F . For example, one can show at all orders of perturbation theory that PQCD predictions reduce to those of an Abelian theory at $N_C \rightarrow 0$ with $\hat{\alpha} = C_F \alpha_s$ and $\widehat{N}_F = N_f/TC_F$ held fixed. In particular, CSRs obey the ‘‘Abelian correspondence principle’’ in that they give the correct Abelian relations at $N_c \rightarrow 0$.

Similarly, commensurate scale relations obey the ‘‘conformal correspondence principle’’: the CSRs reduce to correct conformal relations when N_C and N_F are tuned to produce zero β function. Thus conformal symmetry provides a *template* for QCD predictions, providing relations between observables which are present even in theories which are not scale invariant. All effects of the nonzero beta function are encoded in the appropriate choice of relative scales $\Lambda_{AB} = Q_A/Q_B$.

The scale Q which enters a given effective charge corresponds to a physical momen-

tum scale. The total logarithmic derivative of each effective charge effective charge $\alpha_A(Q)$ with respect to its physical scale is given by the Gell Mann-Low equation:

$$\frac{d\alpha_A(Q, m)}{d \log Q} = \Psi_A(\alpha_A(Q, m), Q/m), \quad (13)$$

where the functional dependence of Ψ_A is specific to its own effective charge. Here m refers to the quark's pole mass. The pole mass is universal in that it does not depend on the choice of effective charge. The Gell Mann-Low relation is reflexive in that ψ_A depends on only on the coupling α_A at the same scale. It should be emphasized that the Gell Mann-Low equation deals with physical quantities and is independent of the renormalization procedure and choice of renormalization scale. A central feature of quantum chromodynamics is asymptotic freedom; *i.e.*, the monotonic decrease of the QCD coupling $\alpha_A(\mu^2)$ at large spacelike scales. The empirical test of asymptotic freedom is the verification of the negative sign of the Gell Mann-Low function at large momentum transfer, which must be true for any effective charge.

In perturbation theory,

$$\Psi_A = -\psi_A^{\{0\}} \frac{\alpha_A^2}{\pi} - \psi_A^{\{1\}} \frac{\alpha_A^3}{\pi^2} - \psi_A^{\{2\}} \frac{\alpha_A^4}{\pi^3} + \dots \quad (14)$$

At large scales $Q^2 \gg m^2$, the first two terms are universal and identical to the first two terms of the β function $\psi_A^{\{0\}} = \beta_0 = \frac{11N_C}{3} - \frac{2}{3}N_F$, $\psi_A^{\{1\}} = \beta_1$, whereas $\psi_A^{\{n\}}$ for $n \geq 2$ is process dependent. The quark mass dependence of the ψ function is analytic, and in the case of α_V scheme is known to two loops.

The commensurate scale relation between α_A and α_B implies an elegant relation between their conformal dependence C_{AB} and their respective Gell Mann Low functions:

$$\psi_B = \frac{dC_{BA}}{d\alpha_A} \times \psi_A. \quad (15)$$

Thus given the result for $N_{F,V}(m/Q)$ in α_V scheme we can use the CSR to derive $N_{F,A}(m/Q)$ for any other effective charge, at least to two loops. The above relation also shows that if one effective charge has a fixed point $\psi_A[\alpha_A(Q_A^{FP})] = 0$, then all effective charges B have a corresponding fixed point $\psi_B[\alpha_B(Q_B^{FP})] = 0$ at the corresponding commensurate scale and value of effective charge.

In quantum electrodynamics, the running coupling $\alpha_{QED}(Q^2)$, defined from the Coulomb scattering of two infinitely heavy test charges at the momentum transfer $t =$

$-Q^2$, is taken as the standard observable. Is there a preferred effective charge which we should use to characterize the coupling strength in QCD? In the case of QCD, the heavy-quark potential $V(Q^2)$ is defined via a Wilson loop from the interaction energy of infinitely heavy quark and antiquark at momentum transfer $t = -Q^2$. The relation $V(Q^2) = -4\pi C_F \alpha_V(Q^2)/Q^2$ then defines the effective charge $\alpha_V(Q)$. As in the corresponding case of Abelian QED, the scale Q of the coupling $\alpha_V(Q)$ is identified with the exchanged momentum. Thus there is never any ambiguity in the interpretation of the scale. All vacuum polarization corrections due to fermion pairs are incorporated in α_V through the usual vacuum polarization kernels which depend on the physical mass thresholds. Other observables could be used to define the standard QCD coupling, such as the effective charge defined from heavy quark radiation [105].

Commensurate scale relations between α_V and the QCD radiative corrections to other observables have no scale or scheme ambiguity, even in multiple-scale problems such as multi-jet production. As is the case in QED, the momentum scale which appears as the argument of α_V reflect the mean virtuality of the exchanged gluons. Furthermore, we can write a commensurate scale relation between α_V and an analytic extension of the \overline{MS} coupling, thus transferring all of the unambiguous scale-fixing and analytic properties of the physical α_V scheme to the \overline{MS} coupling.

An elegant example is the relation between the rate for semi-leptonic B -decay and α_V :

$$\Gamma(b \rightarrow X_u \ell \nu) = \frac{G_F^2 |V_{ub}|^2 M_b^2}{192\pi^3} \left[1 - 2.41 \frac{\alpha_V(0.16 M_b)}{\pi} - 1.43 \frac{\alpha_V(0.16 M_b)^2}{\pi} \right], \quad (16)$$

where M_b is the scheme independent b -quark pole mass. The coefficient of $\alpha_{\overline{MS}}^2(\mu)$ in the usual expansion with $\mu = m_b$ is 26.8.

Some other examples of CSR's at NLO:

$$\alpha_R(\sqrt{s}) = \alpha_{g1}(0.5\sqrt{s}) - \frac{\alpha_{g1}^2(0.5\sqrt{s})}{\pi} + \frac{\alpha_{g1}^3(0.5\sqrt{s})}{\pi^2} \quad (17)$$

$$\alpha_R(\sqrt{s}) = \alpha_V(1.8\sqrt{s}) + 2.08 \frac{\alpha_V^2(1.8\sqrt{s})}{\pi} - 7.16 \frac{\alpha_V^3(1.8\sqrt{s})}{\pi^2} \quad (18)$$

$$\alpha_\tau(\sqrt{s}) = \alpha_V(0.8\sqrt{s}) + 2.08 \frac{\alpha_V^2(0.8\sqrt{s})}{\pi} - 7.16 \frac{\alpha_V^3(0.8\sqrt{s})}{\pi^2} \quad (19)$$

$$\alpha_{g1}(\sqrt{s}) = \alpha_V(0.8Q) + 1.08 \frac{\alpha_V^2(0.8Q)}{\pi} - 10.3 \frac{\alpha_V^3(0.8Q)}{\pi^2} . \quad (20)$$

For numerical purposes in each case we have used $N_F = 5$ and $\alpha_V = 0.1$ to compute the NLO correction to the CSR scale.

Commensurate scale relations thus provide fundamental and precise scheme-independent tests of QCD, predicting how observables track not only in relative normalization, but also in their commensurate scale dependence.

9 The Generalized Crewther Relation

The generalized Crewther relation can be derived by calculating the QCD radiative corrections to the deep inelastic sum rules and $R_{e^+e^-}$ in a convenient renormalization scheme such as the modified minimal subtraction scheme $\overline{\text{MS}}$. One then algebraically eliminates $\alpha_{\overline{\text{MS}}}(\mu)$. Finally, BLM scale-setting [31] is used to eliminate the β -function dependence of the coefficients. The form of the resulting relation between the observables thus matches the result which would have been obtained had QCD been a conformal theory with zero β function. The final result relating the observables is independent of the choice of intermediate $\overline{\text{MS}}$ renormalization scheme.

More specifically, consider the Adler function [106] for the e^+e^- annihilation cross section

$$D(Q^2) = -12\pi^2 Q^2 \frac{d}{dQ^2} \Pi(Q^2), \quad \Pi(Q^2) = -\frac{Q^2}{12\pi^2} \int_{4m_\pi^2}^{\infty} \frac{R_{e^+e^-}(s) ds}{s(s+Q^2)}. \quad (21)$$

The entire radiative correction to this function is defined as the effective charge $\alpha_D(Q^2)$:

$$\begin{aligned} D(Q^2/\mu^2, \alpha_s(\mu^2)) &= D(1, \alpha_s(Q^2)) \\ &\equiv 3 \sum_f Q_f^2 \left[1 + \frac{3}{4} C_F \frac{\alpha_D(Q^2)}{\pi} \right] + (\sum_f Q_f)^2 C_L(Q^2) \\ &\equiv 3 \sum_f Q_f^2 C_D(Q^2) + (\sum_f Q_f)^2 C_L(Q^2), \end{aligned} \quad (22)$$

where $C_F = \frac{N_C^2 - 1}{2N_C}$. The coefficient $C_L(Q^2)$ appears at the third order in perturbation theory and is related to the ‘‘light-by-light scattering type’’ diagrams. (Hereafter α_s will denote the $\overline{\text{MS}}$ scheme strong coupling constant.)

It is straightforward to algebraically relate $\alpha_{g_1}(Q^2)$ to $\alpha_D(Q^2)$ using the known expressions to three loops in the $\overline{\text{MS}}$ scheme. If one chooses the renormalization scale

to resum all of the quark and gluon vacuum polarization corrections into $\alpha_D(Q^2)$, then the final result turns out to be remarkably simple [25] ($\hat{\alpha} = 3/4 C_F \alpha/\pi$) :

$$\hat{\alpha}_{g_1}(Q) = \hat{\alpha}_D(Q^*) - \hat{\alpha}_D^2(Q^*) + \hat{\alpha}_D^3(Q^*) + \dots, \quad (23)$$

where

$$\begin{aligned} \ln\left(\frac{Q^{*2}}{Q^2}\right) = & \frac{7}{2} - 4\zeta(3) + \left(\frac{\alpha_D(Q^*)}{4\pi}\right) \left[\left(\frac{11}{12} + \frac{56}{3}\zeta(3) - 16\zeta^2(3)\right) \beta_0 \right. \\ & \left. + \frac{26}{9}C_A - \frac{8}{3}C_A\zeta(3) - \frac{145}{18}C_F - \frac{184}{3}C_F\zeta(3) + 80C_F\zeta(5) \right]. \end{aligned}$$

where in QCD, $C_A = N_C = 3$ and $C_F = 4/3$. This relation shows how the coefficient functions for these two different processes are related to each other at their respective commensurate scales. We emphasize that the $\overline{\text{MS}}$ renormalization scheme is used only for calculational convenience; it serves simply as an intermediary between observables. The renormalization group ensures that the forms of the CSR relations in perturbative QCD are independent of the choice of an intermediate renormalization scheme.

The Crewther relation was originally derived assuming that the theory is conformally invariant; *i.e.*, for zero β function. In the physical case, where the QCD coupling runs, all non-conformal effects are resummed into the energy and momentum transfer scales of the effective couplings α_R and α_{g_1} . The general relation between these two effective charges for non-conformal theory thus takes the form of a geometric series

$$1 - \hat{\alpha}_{g_1} = [1 + \hat{\alpha}_D(Q^*)]^{-1} . \quad (24)$$

We have dropped the small light-by-light scattering contributions. This is again a special advantage of relating observable to observable. The coefficients are independent of color and are the same in Abelian, non-Abelian, and conformal gauge theory. The non-Abelian structure of the theory is reflected in the expression for the scale Q^* .

Is experiment consistent with the generalized Crewther relation? Fits [107] to the experimental measurements of the R -ratio above the thresholds for the production of $c\bar{c}$ bound states provide the empirical constraint: $\alpha_R(\sqrt{s} = 5.0 \text{ GeV})/\pi \simeq 0.08 \pm 0.03$. The prediction for the effective coupling for the deep inelastic sum rules at the commensurate momentum transfer Q is then $\alpha_{g_1}(Q = 12.33 \pm 1.20 \text{ GeV})/\pi \simeq \alpha_{\text{GLS}}(Q = 12.33 \pm 1.20 \text{ GeV})/\pi \simeq 0.074 \pm 0.026$. Measurements of the Gross-Llewellyn

Smith sum rule have so far only been carried out at relatively small values of Q^2 [108, 109]; however, one can use the results of the theoretical extrapolation [110] of the experimental data presented in [111]: $\alpha_{\text{GLS}}^{\text{extrapol}}(Q = 12.25 \text{ GeV})/\pi \simeq 0.093 \pm 0.042$. This range overlaps with the prediction from the generalized Crewther relation. It is clearly important to have higher precision measurements to fully test this fundamental QCD prediction.

10 General Form of Commensurate Scale Relations

In general, commensurate scale relations connecting the effective charges for observables A and B have the form

$$\alpha_A(Q_A) = \alpha_B(Q_B) \left(1 + r_{A/B}^{(1)} \frac{\alpha_B(Q_B)}{\pi} + r_{A/B}^{(2)} \frac{\alpha_B(Q_B)^2}{\pi} + \dots \right), \quad (25)$$

where the coefficients $r_{A/B}^n$ are identical to the coefficients obtained in a conformally invariant theory with $\beta_B(\alpha_B) \equiv (d/d \ln Q^2) \alpha_B(Q^2) = 0$. The ratio of the scales Q_A/Q_B is thus fixed by the requirement that the couplings sum all of the effects of the non-zero β function. In practice the NLO and NNLO coefficients and relative scales can be identified from the flavor dependence of the perturbative series; *i.e.* by shifting scales such that the N_F -dependence associated with $\beta_0 = 11/3C_A - 4/3T_F N_F$ and $\beta_1 = -34/3C_A^2 + \frac{20}{3}C_A T_F N_F + 4C_F T_F N_F$ does not appear in the coefficients. Here $C_A = N_C$, $C_F = (N_C^2 - 1)/2N_C$ and $T_F = 1/2$. The shift in scales which gives conformal coefficients in effect pre-sums the large and strongly divergent terms in the PQCD series which grow as $n!(\beta_0 \alpha_s)^n$, *i.e.*, the infrared renormalons associated with coupling-constant renormalization [112, 44, 113, 114].

The renormalization scales Q^* in the BLM method are physical in the sense that they reflect the mean virtuality of the gluon propagators. This scale-fixing procedure is consistent with scale fixing in QED, in agreement with in the Abelian limit, $N_C \rightarrow 0$ [31, 28, 115, 116, 117]. The ratio of scales $\lambda_{A/B} = Q_A/Q_B$ guarantees that the observables A and B pass through new quark thresholds at the same physical scale. One can also show that the commensurate scales satisfy the transitivity rule $\lambda_{A/B} = \lambda_{A/C} \lambda_{C/B}$, which ensures that predictions are independent of the choice of an intermediate renormalization scheme or intermediate observable C .

In general, we can write the relation between any two effective charges at arbitrary scales μ_A and μ_B as a correction to the corresponding relation obtained in a conformally invariant theory:

$$\alpha_A(\mu_A) = C_{AB}[\alpha_B(\mu_B)] + \beta_B[\alpha_B(\mu_B)]F_{AB}[\alpha_B(\mu_B)] \quad (26)$$

where

$$C_{AB}[\alpha_B] = \alpha_B + \sum_{n=1} C_{AB}^{(n)} \alpha_B^n \quad (27)$$

is the functional relation when $\beta_B[\alpha_B] = 0$. In fact, if α_B approaches a fixed point $\bar{\alpha}_B$ where $\beta_B[\bar{\alpha}_B] = 0$, then α_A tends to a fixed point given by

$$\alpha_A \rightarrow \bar{\alpha}_A = C_{AB}[\bar{\alpha}_B]. \quad (28)$$

The commensurate scale relation for observables A and B has a similar form, but in this case the relative scales are fixed such that the non-conformal term F_{AB} is zero. Thus the commensurate scale relation $\alpha_A(Q_A) = C_{AB}[\alpha_B(Q_B)]$ at general commensurate scales is also the relation connecting the values of the fixed points for any two effective charges or schemes. Furthermore, as $\beta \rightarrow 0$, the ratio of commensurate scales Q_A^2/Q_B^2 becomes the ratio of fixed point scales \bar{Q}_A^2/\bar{Q}_B^2 as one approaches the fixed point regime.

11 Implementation of α_V Scheme

The effective charge $\alpha_V(Q)$ provides a physically-based alternative to the usual modified minimal subtraction ($\overline{\text{MS}}$) scheme. All vacuum polarization corrections due to fermion pairs are incorporated in α_V through the usual vacuum polarization kernels which depend on the physical mass thresholds. When continued to time-like momenta, the coupling has the correct analytic dependence dictated by the production thresholds in the crossed channel. Since α_V incorporates quark mass effects exactly, it avoids the problem of explicitly computing and resumming quark mass corrections which are related to the running of the coupling. Thus the effective number of flavors $N_F(Q/m)$ is an analytic function of the scale Q and the quark masses m . The effects of finite quark mass corrections on the running of the strong coupling were first considered by De Rújula and Georgi [118] within the momentum subtraction schemes

(MOM) (see also Georgi and Politzer [119], Shirkov and collaborators [120], and Chýla [121]).

One important advantage of the physical charge approach is its inherent gauge invariance to all orders in perturbation theory. This feature is not manifest in massive β -functions defined in non-physical schemes such as the MOM schemes. A second, more practical, advantage is the automatic decoupling of heavy quarks according to the Appelquist-Carazzone theorem [122].

By employing the commensurate scale relations other physical observables can be expressed in terms of the analytic coupling α_V without scale or scheme ambiguity. This way the quark mass threshold effects in the running of the coupling are taken into account by utilizing the mass dependence of the physical α_V scheme. In effect, quark thresholds are treated analytically to all orders in m^2/Q^2 ; *i.e.*, the evolution of the physical α_V coupling in the intermediate regions reflects the actual mass dependence of a physical effective charge and the analytic properties of particle production. Furthermore, the definiteness of the dependence in the quark masses automatically constrains the scale Q in the argument of the coupling. There is thus no scale ambiguity in perturbative expansions in α_V .

In the conventional $\overline{\text{MS}}$ scheme, the coupling is independent of the quark masses since the quarks are treated as either massless or infinitely heavy with respect to the running of the coupling. Thus one formulates different effective theories depending on the effective number of quarks which is governed by the scale Q ; the massless β -function is used to describe the running in between the flavor thresholds. These different theories are then matched to each other by imposing matching conditions at the scale where the effective number of flavors is changed (normally the quark masses). The dependence on the matching scale can be made arbitrarily small by calculating the matching conditions to high enough order. For physical observables one can then include the effects of finite quark masses by making a higher-twist expansion in m^2/Q^2 and Q^2/m^2 for light and heavy quarks, respectively. These higher-twist contributions have to be calculated for each observables separately, so that in principle one requires an all-order resummation of the mass corrections to the effective Lagrangian to give correct results.

The specification of the coupling and renormalization scheme also depends on the definition of the quark mass. In contrast to QED where the on-shell mass provides a

natural definition of lepton masses, an on-shell definition for quark masses is complicated by the confinement property of QCD. In this paper we will use the pole mass $m(p^2 = m^2) = m$ which has the advantage of being scheme and renormalization-scale invariant. Furthermore, when combined with the α_V scheme, the pole mass gives predictions which are free of the leading renormalon ambiguity.

A technical complication of massive schemes is that one cannot easily obtain analytic solutions of renormalization group equations to the massive β function, and the Gell-Mann Low function is scheme-dependent even at lowest order.

In a recent paper we have presented a two-loop analytic extension of the α_V -scheme based on the recent results of Ref. [123]. The mass effects are in principle treated exactly to two-loop order and are only limited in practice by the uncertainties from numerical integration. The desired features of gauge invariance and decoupling are manifest in the form of the two-loop Gell-Mann Low function, and we give a simple fitting-function which interpolates smoothly the exact two-loop results obtained by using the adoptive Monte Carlo integrator VEGAS [124]. Strong consistency checks of the results are performed by comparing the Abelian limit to the well known QED results in the on-shell scheme. In addition, the massless as well as the decoupling limit are reproduced exactly, and the two-loop Gell-Mann Low function is shown to be renormalization scale independent.

The results of our numerical calculation of $N_{F,V}^{(1)}$ in the V -scheme for QCD and QED are shown in Fig. 3. The decoupling of heavy quarks becomes manifest at small Q/m , and the massless limit is attained for large Q/m . The QCD form actually becomes negative at moderate values of Q/m , a novel feature of the anti-screening non-Abelian contributions. This property is also present in the (gauge dependent) MOM results. In contrast, in Abelian QED the two-loop contribution to the effective number of flavors becomes larger than 1 at intermediate values of Q/m . We also display the one-loop contribution $N_{F,V}^{(0)}\left(\frac{Q}{m}\right)$ which monotonically interpolates between the decoupling and massless limits. The solid curves displayed in Fig. 3 shows that the parameterizations which we used for fitting the numerical results are quite accurate.

The relation of $\alpha_V(Q^2)$ to the conventional \overline{MS} coupling is now known to NNLO [125], but for clarity in this section only the NLO relation will be used. The com-

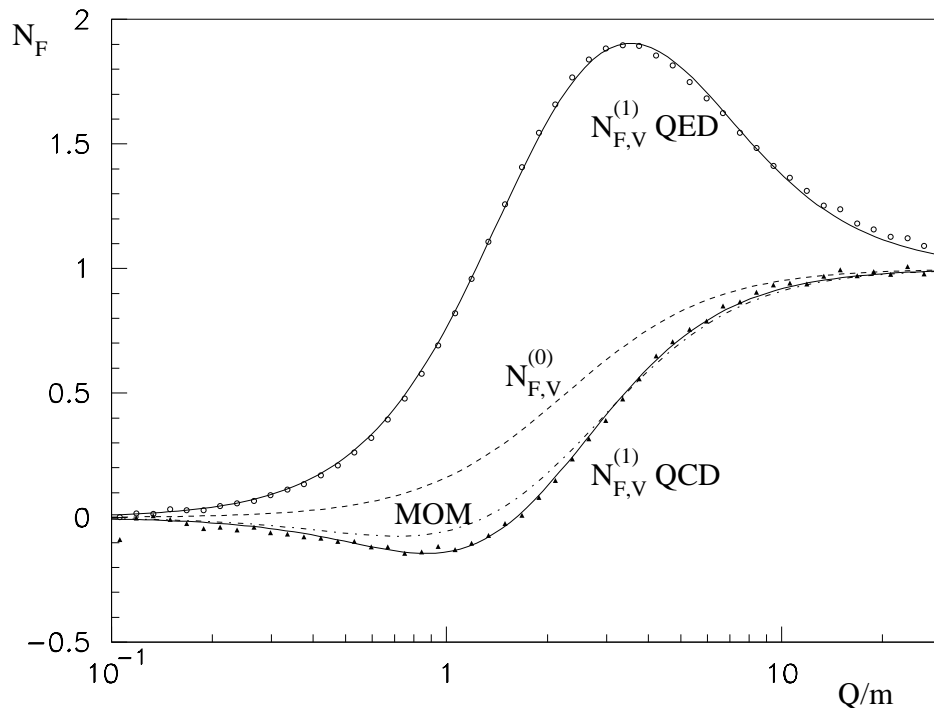


Figure 3: The numerical results for the gauge-invariant $N_{F,V}^{(1)}$ in QED (open circles) and QCD (triangles) with the best χ^2 fits superimposed respectively. The dashed line shows the one-loop $N_{F,V}^{(0)}$ function. For comparison we also show the gauge dependent two-loop result obtained in MOM schemes (dash-dot) [127, 128]. At large $\frac{Q}{m}$ the theory becomes effectively massless, and both schemes agree as expected. The figure also illustrates the decoupling of heavy quarks at small $\frac{Q}{m}$.

mensurate scale relation is given by [126]

$$\begin{aligned}
 \alpha_{\overline{\text{MS}}}(Q) &= \alpha_V(Q^*) + \frac{2}{3} N_C \frac{\alpha_V^2(Q^*)}{\pi} \\
 &= \alpha_V(Q^*) + 2 \frac{\alpha_V^2(Q^*)}{\pi},
 \end{aligned}
 \tag{29}$$

which is valid for $Q^2 \gg m^2$. The coefficients in the perturbation expansion have their conformal values, *i.e.*, the same coefficients would occur even if the theory had been conformally invariant with $\beta = 0$. The commensurate scale is given by

$$Q^* = Q \exp \left[\frac{5}{6} \right].
 \tag{30}$$

The scale in the \overline{MS} scheme is thus a factor ~ 0.4 smaller than the physical scale. The coefficient $2N_C/3$ in the NLO coefficient is a feature of the non-Abelian couplings of QCD; the same coefficient occurs even if the theory were conformally invariant with $\beta_0 = 0$.

Using the above QCD results, we can transform any NLO prediction given in \overline{MS} scheme to a scale-fixed expansion in $\alpha_V(Q)$. We can also derive the connection between the \overline{MS} and α_V schemes for Abelian perturbation theory using the limit $N_C \rightarrow 0$ with $C_F\alpha_s$ and N_F/C_F held fixed [28].

The use of α_V and related physically defined effective charges such as α_p (to NLO the effective charge defined from the (1,1) plaquette, α_p is the same as α_V) as expansion parameters has been found to be valuable in lattice gauge theory, greatly increasing the convergence of perturbative expansions relative to those using the bare lattice coupling [115]. Recent lattice calculations of the Υ - spectrum [129] have been used with BLM scale-fixing to determine a NLO normalization of the static heavy quark potential: $\alpha_V^{(3)}(8.2\text{GeV}) = 0.196(3)$ where the effective number of light flavors is $n_f = 3$. The corresponding modified minimal subtraction coupling evolved to the Z mass and five flavors is $\alpha_{\overline{MS}}^{(5)}(M_Z) = 0.1174(24)$. Thus a high precision value for $\alpha_V(Q^2)$ at a specific scale is available from lattice gauge theory. Predictions for other QCD observables can be directly referenced to this value without the scale or scheme ambiguities, thus greatly increasing the precision of QCD tests.

One can also use α_V to characterize the coupling which appears in the hard scattering contributions of exclusive process amplitudes at large momentum transfer, such as elastic hadronic form factors, the photon-to-pion transition form factor at large momentum transfer [31, 32] and exclusive weak decays of heavy hadrons [13]. Each gluon propagator with four-momentum k^μ in the hard-scattering quark-gluon scattering amplitude T_H can be associated with the coupling $\alpha_V(k^2)$ since the gluon exchange propagators closely resembles the interactions encoded in the effective potential $V(Q^2)$. [In Abelian theory this is exact.] Commensurate scale relations can then be established which connect the hard-scattering subprocess amplitudes which control exclusive processes to other QCD observables.

We can anticipate that eventually nonperturbative methods such as lattice gauge theory or discretized light-cone quantization will provide a complete form for the heavy quark potential in QCD . It is reasonable to assume that $\alpha_V(Q)$ will not diverge

at small space-like momenta. One possibility is that α_V stays relatively constant $\alpha_V(Q) \simeq 0.4$ at low momenta, consistent with fixed-point behavior. There is, in fact, empirical evidence for freezing of the α_V coupling from the observed systematic dimensional scaling behavior of exclusive reactions [32]. If this is in fact the case, then the range of QCD predictions can be extended to quite low momentum scales, a regime normally avoided because of the apparent singular structure of perturbative extrapolations.

There are a number of other advantages of the V -scheme:

1. Perturbative expansions in α_V with the scale set by the momentum transfer cannot have any β -function dependence in their coefficients since all running coupling effects are already summed into the definition of the potential. Since coefficients involving β_0 cannot occur in an expansions in α_V , the divergent infrared renormalon series of the form $\alpha_V^n \beta_0^n n!$ cannot occur. The general convergence properties of the scale Q^* as an expansion in α_V is not known [44].
2. The effective coupling $\alpha_V(Q^2)$ incorporates vacuum polarization contributions with finite fermion masses. When continued to time-like momenta, the coupling has the correct analytic dependence dictated by the production thresholds in the t channel. Since α_V incorporates quark mass effects exactly, it avoids the problem of explicitly computing and resumming quark mass corrections.
3. The α_V coupling is the natural expansion parameter for processes involving non-relativistic momenta, such as heavy quark production at threshold where the Coulomb interactions, which are enhanced at low relative velocity v as $\pi\alpha_V/v$, need to be re-summed [130, 131, 132]. The effective Hamiltonian for nonrelativistic QCD is thus most naturally written in α_V scheme. The threshold corrections to heavy quark production in e^+e^- annihilation depend on α_V at specific scales Q^* . Two distinct ranges of scales arise as arguments of α_V near threshold: the relative momentum of the quarks governing the soft gluon exchange responsible for the Coulomb potential, and a high momentum scale, induced by hard gluon exchange, approximately equal to twice the quark mass for the corrections [131]. One thus can use threshold production to obtain a direct determination of α_V even at low scales. The corresponding QED results

for τ pair production allow for a measurement of the magnetic moment of the τ and could be tested at a future τ -charm factory [130, 131].

We also note that computations in different sectors of the Standard Model have been traditionally carried out using different renormalization schemes. However, in a grand unified theory, the forces between all of the particles in the fundamental representation should become universal above the grand unification scale. Thus it is natural to use α_V as the effective charge for all sectors of a grand unified theory, rather than in a convention-dependent coupling such as $\alpha_{\overline{MS}}$.

12 Extension of the \overline{MS} Scheme

The standard \overline{MS} scheme is not an analytic function of the renormalization scale at heavy quark thresholds; in the running of the coupling the quarks are taken as massless, and at each quark threshold the value of N_F which appears in the β function is incremented. Thus Eq. (29) is technically only valid far above a heavy quark threshold. However, we can use this commensurate scale relation to define an extended \overline{MS} scheme which is continuous and analytic at any scale. The new modified scheme inherits all of the good properties of the α_V scheme, including its correct analytic properties as a function of the quark masses and its unambiguous scale fixing [126]. Thus we define

$$\tilde{\alpha}_{\overline{MS}}(Q) = \alpha_V(Q^*) + \frac{2N_C}{3} \frac{\alpha_V^2(Q^{**})}{\pi} + \dots, \quad (31)$$

for all scales Q . This equation not only provides an analytic extension of the \overline{MS} and similar schemes, but it also ties down the renormalization scale to the physical masses of the quarks as they enter into the vacuum polarization contributions to α_V .

The modified scheme $\tilde{\alpha}_{\overline{MS}}$ provides an analytic interpolation of conventional \overline{MS} expressions by utilizing the mass dependence of the physical α_V scheme. In effect, quark thresholds are treated analytically to all orders in m^2/Q^2 ; *i.e.*, the evolution of the analytically extended coupling in the intermediate regions reflects the actual mass dependence of a physical effective charge and the analytic properties of particle production. Just as in Abelian QED, the mass dependence of the effective potential and the analytically extended scheme $\tilde{\alpha}_{\overline{MS}}$ reflects the analyticity of the physical thresholds for particle production in the crossed channel. Furthermore, the definiteness

of the dependence in the quark masses automatically constrains the renormalization scale. There is thus no scale ambiguity in perturbative expansions in α_V or $\tilde{\alpha}_{\overline{\text{MS}}}$.

In leading order the effective number of flavors in the modified scheme $\tilde{\alpha}_{\overline{\text{MS}}}$ is given to a very good approximation by the simple form [126]

$$\tilde{N}_{F,\overline{\text{MS}}}^{(0)}\left(\frac{m^2}{Q^2}\right) \cong \left(1 + \frac{5m^2}{Q^2 \exp(\frac{5}{3})}\right)^{-1} \cong \left(1 + \frac{m^2}{Q^2}\right)^{-1}. \quad (32)$$

Thus the contribution from one flavor is $\simeq 0.5$ when the scale Q equals the quark mass m_i . The standard procedure of matching $\alpha_{\overline{\text{MS}}}(\mu)$ at the quark masses serves as a zeroth-order approximation to the continuous N_F .

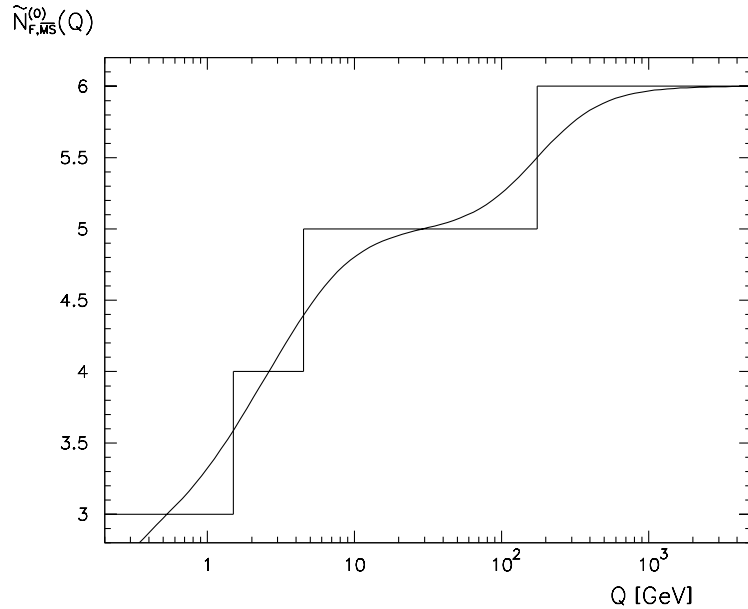


Figure 4: The continuous $\tilde{N}_{F,\overline{\text{MS}}}^{(0)}$ in the analytic extension of the $\overline{\text{MS}}$ scheme as a function of the physical scale Q . (For reference the continuous N_F is also compared with the conventional procedure of taking N_F to be a step-function at the quark-mass thresholds.)

Adding all flavors together gives the total $\tilde{N}_{F,\overline{\text{MS}}}^{(0)}(Q)$ which is shown in Fig. 4. For reference, the continuous N_F is also compared with the conventional procedure of taking N_F to be a step-function at the quark-mass thresholds. The figure shows clearly that there are hardly any plateaus at all for the continuous $\tilde{N}_{F,\overline{\text{MS}}}^{(0)}(Q)$ in between

the quark masses. Thus there is really no scale below 1 TeV where $\widetilde{N}_{F,\overline{\text{MS}}}^{(0)}(Q)$ can be approximated by a constant; for all Q below 1 TeV there is always one quark with mass m_i such that $m_i^2 \ll Q^2$ or $Q^2 \gg m_i^2$ is not true. We also note that if one would use any other scale than the BLM-scale for $\widetilde{N}_{F,\overline{\text{MS}}}^{(0)}(Q)$, the result would be to increase the difference between the analytic N_F and the standard procedure of using the step-function at the quark-mass thresholds.

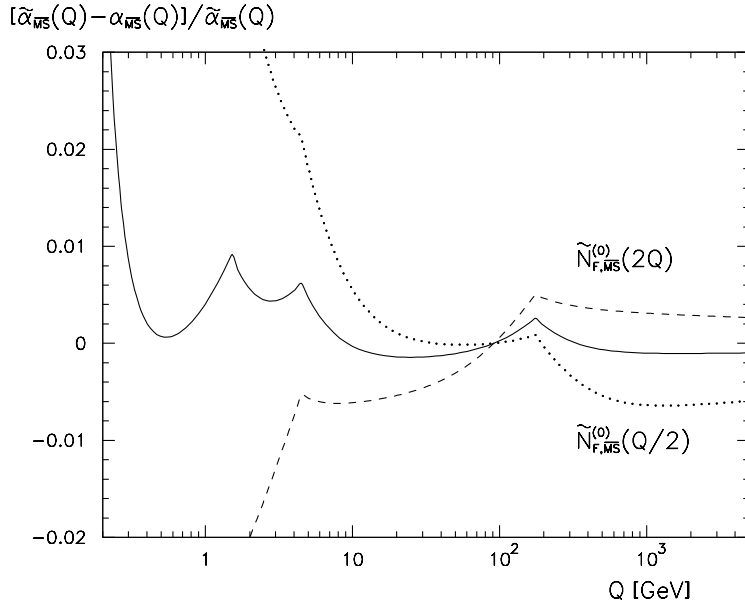


Figure 5: The solid curve shows the relative difference between the solutions to the 1-loop renormalization group equation using continuous N_F , $\widetilde{\alpha}_{\overline{\text{MS}}}(Q)$, and conventional discrete theta-function thresholds, $\alpha_{\overline{\text{MS}}}(Q)$. The dashed (dotted) curves shows the same quantity but using the scale $2Q$ ($Q/2$) in $\widetilde{N}_{F,\overline{\text{MS}}}^{(0)}$. The solutions have been obtained numerically starting from the world average [133] $\alpha_{\overline{\text{MS}}}(M_Z) = 0.118$.

Figure 5 shows the relative difference between the two different solutions of the 1-loop renormalization group equation, *i.e.* $(\widetilde{\alpha}_{\overline{\text{MS}}}(Q) - \alpha_{\overline{\text{MS}}}(Q)) / \widetilde{\alpha}_{\overline{\text{MS}}}(Q)$. The solutions have been obtained numerically starting from the world average [133] $\alpha_{\overline{\text{MS}}}(M_Z) = 0.118$. The figure shows that taking the quark masses into account in the running leads to effects of the order of one percent which are most especially pronounced near thresholds.

The extension of the $\overline{\text{MS}}$ -scheme proposed here provides a coupling which is an analytic function of both the scale and the quark masses. The new modified coupling $\tilde{\alpha}_{\overline{\text{MS}}}(Q)$ inherits most of the good properties of the α_V scheme, including its correct analytic properties as a function of the quark masses and its unambiguous scale fixing [126]. However, the conformal coefficients in the commensurate scale relation between the α_V and $\overline{\text{MS}}$ schemes does not preserve one of the defining criterion of the potential expressed in the bare charge, namely the non-occurrence of color factors corresponding to an iteration of the potential. This is probably an effect of the breaking of conformal invariance by the $\overline{\text{MS}}$ scheme. The breaking of conformal symmetry has also been observed when dimensional regularization is used as a factorization scheme in both exclusive [77, 134, 135] and inclusive [136] reactions. Thus, it does not turn out to be possible to extend the modified scheme $\tilde{\alpha}_{\overline{\text{MS}}}$ beyond leading order without running into an intrinsic contradiction with conformal symmetry.

The observation of rapidly increasing structure functions in deep inelastic scattering at small- x_{bj} and the observation of rapidly increasing diffractive processes such as $\gamma^*p \rightarrow \rho p$ at high energies at HERA is in agreement with the expectations of the BFKL [137] QCD high-energy limit. The highest eigenvalue, ω^{max} , of the leading order (LO) BFKL equation [137] is related to the intercept of the Pomeron which in turn governs the high-energy asymptotics of the cross sections: $\sigma \sim s^{\alpha_{IP}-1} = s^{\omega^{\text{max}}}$. The BFKL Pomeron intercept in LO turns out to be rather large: $\alpha_{IP} - 1 = \omega_L^{\text{max}} = 12 \ln 2 (\alpha_S/\pi) \simeq 0.55$ for $\alpha_S = 0.2$; hence, it is very important to know the next-to-leading order (NLO) corrections.

Recently the NLO corrections to the BFKL resummation of energy logarithms were calculated [138, 139] by employing the modified minimal subtraction scheme ($\overline{\text{MS}}$) [140] to regulate the ultraviolet divergences with arbitrary scale setting. The NLO corrections [138, 139] to the highest eigenvalue of the BFKL equation turn out to be negative and even larger than the LO contribution for $\alpha_s > 0.157$. It is thus important to analyze the NLO BFKL resummation of energy logarithms [138, 139] in physical renormalization schemes and apply the BLM-CSR method. In fact, as shown in a recent paper [141], the reliability of QCD predictions for the intercept of the BFKL Pomeron at NLO when evaluated using BLM scale setting [31] within non-Abelian physical schemes, such as the momentum space subtraction (MOM) scheme [142, 143] or the Υ -scheme based on $\Upsilon \rightarrow ggg$ decay, is significantly improved

compared to the $\overline{\text{MS}}$ -scheme.

The renormalization scale ambiguity problem can be resolved if one can optimize the choice of scales and renormalization schemes according to some sensible criteria. In the BLM optimal scale setting [31], the renormalization scales are chosen such that all vacuum polarization effects from the QCD β -function are resummed into the running couplings. The coefficients of the perturbative series are thus identical to the perturbative coefficients of the corresponding conformally invariant theory with $\beta = 0$.

In the present case one can show that within the V-scheme (or the $\overline{\text{MS}}$ -scheme) the BLM procedure does not change significantly the value of the NLO coefficient $r(\nu)$. This can be understood since the V-scheme, as well as $\overline{\text{MS}}$ -scheme, are adjusted primarily to the case when in the LO there are dominant QED (Abelian) type contributions, whereas in the BFKL case there are important LO gluon-gluon (non-Abelian) interactions. Thus one can choose for the BFKL case the MOM-scheme [142, 143] or the Υ -scheme based on $\Upsilon \rightarrow ggg$ decay.

Adopting BLM scale setting, the NLO BFKL eigenvalue in the MOM-scheme is

$$\omega_{BLM}^{MOM}(Q^2, \nu) = N_C \chi_L(\nu) \frac{\alpha_{MOM}(Q_{BLM}^{MOM^2})}{\pi} \left[1 + r_{BLM}^{MOM}(\nu) \frac{\alpha_{MOM}(Q_{BLM}^{MOM^2})}{\pi} \right], \quad (33)$$

$$r_{BLM}^{MOM}(\nu) = r_{MOM}^{conf}(\nu).$$

The β -dependent part of the $r_{MOM}(\nu)$ defines the corresponding BLM optimal scale

$$Q_{BLM}^{MOM^2}(\nu) = Q^2 \exp \left[-\frac{4r_{MOM}^\beta(\nu)}{\beta_0} \right] = Q^2 \exp \left[\frac{1}{2} \chi_L(\nu) - \frac{5}{3} + 2 \left(1 + \frac{2}{3} I \right) \right]. \quad (34)$$

At $\nu = 0$ we have $Q_{BLM}^{MOM^2}(0) = Q^2 (4 \exp[2(1 + 2I/3)] - 5/3) \simeq Q^2 127$. Note that $Q_{BLM}^{MOM^2}(\nu)$ contains a large factor, $\exp[-4T_{MOM}^\beta/\beta_0] = \exp[2(1 + 2I/3)] \simeq 168$, which reflects a large kinematic difference between MOM- and $\overline{\text{MS}}$ - schemes [144, 31].

One of the striking features of this analysis is that the NLO value for the intercept of the BFKL Pomeron, improved by the BLM procedure, has a very weak dependence on the gluon virtuality Q^2 . This agrees with the conventional Regge-theory where one expects an universal intercept of the Pomeron without any Q^2 -dependence. The minor Q^2 -dependence obtained, on one side, provides near insensitivity of the results to the precise value of Λ , and, on the other side, leads to approximate scale and conformal

invariance. Thus one may use conformal symmetry [145, 146] for the continuation of the present results to the case $t \neq 0$.

The NLO corrections to the BFKL equation for the QCD Pomeron thus become controllable and meaningful provided one uses physical renormalization scales and schemes relevant to non-Abelian gauge theory. BLM optimal scale setting automatically sets the appropriate physical renormalization scale by absorbing the non-conformal β -dependent coefficients. The strong renormalization scheme dependence of the NLO corrections to BFKL resummation then largely disappears. This is in contrast to the unstable NLO results obtained in the conventional $\overline{\text{MS}}$ -scheme with arbitrary choice of renormalization scale. A striking feature of the NLO BFKL Pomeron intercept in the BLM approach is its very weak Q^2 -dependence, which provides approximate conformal invariance.

The new results presented here open new windows for applications of NLO BFKL resummation to high-energy phenomenology.

Recently the *L3* collaboration at LEPL3 has presented new results for the virtual photon cross section $\sigma(\gamma^*(Q_A)\gamma^*(Q_b) \rightarrow \text{hadrons})$ using double tagged $e^+e^- \rightarrow e^+e^- \text{hadrons}$. This process provides a remarkably clean possible test of the perturbative QCD pomeron since there are no initial hadrons [147]. The calculation of $\sigma(\gamma^*\gamma^*)$ and is discussed in detail in references [147]. We note here some important features:

i) for large virtualities, $\sigma(\gamma^*\gamma^*)$ the longitudinal cross section σ_{LL} dominates and scales like $1/Q^2$, where $Q^2 \sim \max\{Q_A^2, Q_B^2\}$. This is characteristic of the perturbative QCD prediction. Models based on Regge factorization (which work well in the soft-interaction regime dominating $\gamma\gamma$ scattering near the mass shell) would predict a higher power in $1/Q$.

ii) $\sigma(\gamma^*\gamma^*)$ is affected by logarithmic corrections in the energy s to all orders in α_s . As a result of the BFKL summation of these contributions, the cross section rises like a power in s , $\sigma \propto s^\lambda$. The Born approximation to this result (that is, the $\mathcal{O}(\alpha_s^2)$ contribution, corresponding to single gluon exchange gives a constant cross section, $\sigma_{\text{Born}} \propto s^0$. A fit to photon-photon sub-energy dependence measured by L3 at $\sqrt{s_{e^+e^-}} = 91 \text{ GeV}$ and $\langle Q_A^2 \rangle = \langle Q_B^2 \rangle = 3.5 \text{ GeV}^2$ gives $\alpha_P - 1 = 0.28 \pm 0.05$. The L3 data at $\sqrt{s_{e^+e^-}} = 183 \text{ GeV}$ and $\langle Q_A^2 \rangle = \langle Q_B^2 \rangle = 14 \text{ GeV}^2$, gives $\alpha_P - 1 = 0.40 \pm 0.07$ which shows a rise of the virtual photon cross section much stronger than single gluon or soft pomeron exchange, but it is compatible with the expectations from the NLO

scale- and scheme-fixed BFKL predictions. It will be crucial to measure the Q_A^2 and Q_B^2 scaling and polarization dependence and compare with the detailed predictions of PQCD [147].

Commensurate scale relations have a number of attractive properties:

1. The ratio of physical scales Q_A/Q_B which appears in commensurate scale relations reflects the relative position of physical thresholds, *i.e.* quark anti-quark pair production.
2. The functional dependence and perturbative expansion of the CSR are identical to those of a conformal scale-invariant theory where $\beta_A(\alpha_A) = 0$ and $\beta_B(\alpha_B) = 0$.
3. In the case of theories approaching fixed-point behavior $\beta_A(\bar{\alpha}_A) = 0$ and $\beta_B(\bar{\alpha}_B) = 0$, the commensurate scale relation relates both the ratio of fixed point couplings $\bar{\alpha}_A/\bar{\alpha}_B$, and the ratio of scales as the fixed point is approached.
4. Commensurate scale relations satisfy the Abelian correspondence principle [28]; the non-Abelian gauge theory prediction reduces to Abelian theory for $N_C \rightarrow 0$ at fixed $C_F\alpha_s$ and fixed N_F/C_F .
5. The perturbative expansion of a commensurate scale relation has the same form as a conformal theory, and thus has no $n!$ renormalon growth arising from the β -function [148]. It is an interesting conjecture whether the perturbative expansion relating observables to observable are in fact free of all $n!$ growth. The generalized Crewther relation, where the commensurate relation's perturbative expansion forms a geometric series to all orders, has convergent behavior.

Virtually any perturbative QCD prediction can be written in the form of a commensurate scale relation, thus eliminating any uncertainty due to renormalization scheme or scale dependence. Recently it has been shown [149] how the commensurate scale relation between the radiative corrections to τ -lepton decay and $R_{e^+e^-}(s)$ can be generalized and empirically tested for arbitrary τ mass and nearly arbitrarily functional dependence of the τ weak decay matrix element.

An essential feature of the $\alpha_V(Q)$ scheme is the absence of any renormalization scale ambiguity, since Q^2 is, by definition, the square of the physical momentum

transfer. The α_V scheme naturally takes into account quark mass thresholds, which is of particular phenomenological importance to QCD applications in the mass region close to threshold. As we have seen, commensurate scale relations provide an analytic extension of the conventional $\overline{\text{MS}}$ scheme in which many of the advantages of the α_V scheme are inherited by the $\tilde{\alpha}_{\overline{\text{MS}}}$ scheme, but only minimal changes have to be made. Given the commensurate scale relation connecting $\tilde{\alpha}_{\overline{\text{MS}}}$ to α_V expansions in $\tilde{\alpha}_{\overline{\text{MS}}}$ are effectively expansions in α_V to the given order in perturbation theory at a corresponding commensurate scale.

The calculation of $\psi_V^{(1)}$, the two-loop term in the Gell-Mann Low function for the α_V scheme, with massive quarks gives for the first time a gauge invariant and renormalization scheme independent two-loop result for the effects of quarks masses in the running of the coupling. Renormalization scheme independence is achieved by using the pole mass definition for the “light” quarks which contribute to the scale dependence of the static heavy quark potential. Thus the pole mass and the V -scheme are closely connected and have to be used in conjunction to give reasonable results.

It is interesting that the effective number of flavors in the two-loop coefficient of the Gell-Mann Low function in the α_V scheme, $N_{F,V}^{(1)}$, becomes negative for intermediate values of Q/m . This feature can be understood as anti-screening from the non-Abelian contributions and should be contrasted with the QED case where the effective number of flavors becomes larger than 1 for intermediate Q/m . For small Q/m the heavy quarks decouple explicitly as expected in a physical scheme, and for large Q/m the massless result is retained.

The analyticity of the α_V coupling can be utilized to obtain predictions for any perturbatively calculable observables including the finite quark mass effects associated with the running of the coupling. By employing the commensurate scale relation method, observables which have been calculated in the $\overline{\text{MS}}$ scheme can be related to the analytic V -scheme without any scale ambiguity. The commensurate scale relations provides the relation between the physical scales of two effective charges where they pass through a common flavor threshold. We also note the utility of the α_V effective charge in supersymmetric and grand unified theories, particularly since the unification of couplings and masses would be expected to occur in terms of physical quantities rather than parameters defined by theoretical convention.

As an example we have showed in Ref. [126] how to calculate the finite quark mass

corrections connected with the running of the coupling for the non-singlet hadronic width of the Z-boson compared with the standard treatment in the $\overline{\text{MS}}$ scheme. The analytic treatment in the V-scheme gives a simple and straightforward way of incorporating these effects for any observable. This should be contrasted with the $\overline{\text{MS}}$ scheme where higher twist corrections due to finite quark mass threshold effects have to be calculated separately for each observable. The V-scheme is especially suitable for problems where the quark masses are important such as for threshold production of heavy quarks and the hadronic width of the τ lepton.

It has also been shown that the NLO corrections to the BFKL equation for the QCD Pomeron become controllable and meaningful provided one uses physical renormalization scales and schemes relevant to non-Abelian gauge theory. BLM optimal scale setting automatically sets the appropriate physical renormalization scale by absorbing the non-conformal β -dependent coefficients. The strong renormalization scheme dependence of the NLO corrections to BFKL resummation then largely disappears. This is in contrast to the unstable NLO results obtained in the conventional $\overline{\text{MS}}$ -scheme with arbitrary choice of renormalization scale. A striking feature of the NLO BFKL Pomeron intercept in the BLM/CSR approach is its very weak Q^2 -dependence, which provides approximate conformal invariance. The new results presented here open new windows for applications of NLO BFKL resummation to high-energy phenomenology, particularly virtual photon-photon scattering.

Outlook

The traditional focus of theoretical work in QCD has been on hard inclusive processes and jet physics where perturbative methods and leading-twist factorization provide predictions up to next-to-next-to leading order. Most of these predictions appear to be validated by experiment with good precision. More recently, the domain of reliable perturbative QCD predictions has been extended to much more complex phenomena, such as the BFKL approach to the hard QCD pomeron in deep inelastic scattering at small x_{bj} , [150] virtual photon scattering [151], and the energy dependence of hard virtual photon diffractive processes, such as $\gamma^*p \rightarrow \rho^0p$ [42].

Exclusive hard-scattering reactions and hard diffractive reactions are now providing an invaluable window into the structure and dynamics of hadronic amplitudes.

Recent measurements of the photon-to-pion transition form factor at CLEO [75], the diffractive dissociation of pions into jets at Fermilab [76], diffractive vector meson leptonproduction at Fermilab and HERA, and the new program of experiments on exclusive proton and deuteron processes at Jefferson Laboratory are now yielding fundamental information on hadronic wavefunctions, particularly the distribution amplitude of mesons. There is now strong evidence for color transparency from such processes. Such information is also critical for interpreting exclusive heavy hadron decays and the matrix elements and amplitudes entering CP -violating processes at the B factories.

It many ways the study of quantum chromodynamics is just beginning. The most important features of the theory remain to be solved, such as the problem of confinement in QCD, the behavior of the QCD coupling in the infrared, the phase and vacuum structure/zero mode structure of QCD, the fundamental understanding of hadronization and parton coalescence at the amplitude level, and the nonperturbative structure of hadron wavefunctions. There are also still many outstanding phenomenological puzzles in QCD. The precise interpretation of CP violation and the weak interaction parameters in exclusive B decays will require a full understanding of the QCD physics of hadrons.

Light-cone quantization methods appear to be especially well suited for progress in understanding the relevant nonperturbative structure of the theory. Since the Hamiltonian approach is formulated in Minkowski space, predictions for the hadronic phases needed for CP violation studies can be obtained. In these lectures I have discussed how light-cone Fock-state wavefunctions can be used to encode the properties of a hadron in terms of its fundamental quark and gluon degrees of freedom. Given the proton's light-cone wavefunctions, one can compute not only the quark and gluon distributions measured in deep inelastic lepton-proton scattering, but also the multiparton correlations which control helicity correlations in polarized leptonproduction [152], the distribution of particles in the proton fragmentation region and dynamical higher twist effects. Light-cone wavefunctions also provide a systematic framework for evaluating exclusive hadronic matrix elements, including timelike heavy hadron decay amplitudes and form factors.

Commensurate scale relations promise a new level of precision in perturbative QCD predictions which are devoid of renormalization scale and renormalon ambi-

guities. However, progress in QCD is driven by experiment, and we are fortunate that there are new experimental facilities such as Jefferson laboratory, the upcoming QCD studies of exclusive processes e^+e^- and $\gamma\gamma$ processes at the high luminosity B factories, as well as the new accelerators and colliders now being planned to further advance the study of QCD phenomena.

Acknowledgments

Work supported by the Department of Energy, contract DE-AC03-76SF00515. Many of the results presented here are based on collaborations with a number of colleagues, including Steven Bass, Victor Fadin, Gregory Gabadadze, Mandeep Gill, John Hiller, Paul Hoyer, Markus Diehl. Dae Sung Hwang, Chueng Ji, Andrei Kataev, Victor Kim, Peter Lepage, Lev Lipatov, Hung Jung Lu, Gary McCartor, Michael Melles, Chris Pauli, Stephane Peigne, Grigori B. Pivovarov, Johan Rathsman, Ivan Schmidt, and Prem Srivastava. I thank S. Dalley, Yitzhak Frishman, Einan Gardi, Georges Grunberg, Paul Hoyer, Marek Karliner, Carlos Merino, Al Mueller, and Jose Pelaez for helpful conversations. Parts of these lectures were also presented at the 12th Nuclear Physics Summer School and Symposium (NUSS '99). The section on commensurate scale relations is based on a review written in collaboration with Johan Rathsman [26]. I especially thank Piet Mulders and his colleagues for their outstanding hospitality in Nijmegen.

APPENDIX I

LIGHT CONE QUANTIZATION AND PERTURBATION THEORY

In this Appendix, the canonical quantization of QCD in the ghost free $A^+ = 0$ light-cone gauge is given. The discussion follows that given in Refs. [153, 99, 154]. The light-cone quantization of QCD in Feynman gauge is given in Ref. [21] The quantization proceeds in several steps. First one identifies the independent dynamical degrees of freedom in the Lagrangian. The theory is quantized by defining commutation relations for these dynamical fields at a given light-cone time $\tau = t + z$ (we choose $\tau = 0$). These commutation relations lead immediately to the definition of the Fock state basis. Expressing dependent fields in terms of the independent fields, we then derive a light-cone Hamiltonian, which determines the evolution of the state space

with changing τ . Finally the rules for τ -ordered perturbation theory are given. The major purpose of this exercise is to illustrate the origins and nature of the Fock state expansion, and of light-cone perturbation theory. Subtleties due to the large scale structure of non-Abelian gauge fields (*e.g.* ‘instantons’), chiral symmetry breaking, and the like are ignored. Although these have a profound effect on the structure of the vacuum, the theory can still be described with a Fock state basis and some sort of effective Hamiltonian. Furthermore, the short distance interactions of the theory are unaffected by this structure, or at least this is the central ansatz of perturbative QCD.

Quantization

The Lagrangian (density) for QCD can be written

$$\mathcal{L} = -\frac{1}{2} \text{Tr} (F^{\mu\nu} F_{\mu\nu}) + \bar{\psi} (i \not{D} - m) \psi \quad (35)$$

where $F^{\mu\nu} = \partial^\mu A^\nu - \partial^\nu A^\mu + ig[A^\mu, A^\nu]$ and $iD^\mu = i\partial^\mu - gA^\mu$. Here the gauge field A^μ is a traceless 3×3 color matrix ($A^\mu \equiv \sum_a A^{a\mu} T^a$, $\text{Tr}(T^a T^b) = 1/2\delta^{ab}$, $[T^a, T^b] = ic^{abc}T^c, \dots$), and the quark field ψ is a color triplet spinor (for simplicity, we include only one flavor). At a given light-cone time, say $\tau = 0$, the independent dynamical fields are $\psi_\pm \equiv \Lambda_\pm \psi$ and A_\perp^i with conjugate fields $i\psi_\pm^\dagger$ and $\partial^+ A_\perp^i$, where $\Lambda_\pm = \gamma^o \gamma^\pm / 2$ are projection operators ($\Lambda_+ \Lambda_- = 0$, $\Lambda_\pm^2 = \Lambda_\pm$, $\Lambda_+ + \Lambda_- = 1$) and $\partial^\pm = \partial^0 \pm \partial^3$. Using the equations of motion, the remaining fields in \mathcal{L} can be expressed in terms of ψ_+ , A_\perp^i :

$$\begin{aligned} \psi_- &\equiv \Lambda_- \psi = \frac{1}{i\partial^+} [i\vec{D}_\perp \cdot \vec{\alpha}_\perp + \beta m] \psi_+ \\ &= \tilde{\psi}_- - \frac{1}{i\partial^+} g \vec{A}_\perp \cdot \vec{\alpha}_\perp \psi_+ , \\ A^+ &= 0 , \\ A^- &= \frac{2}{i\partial^+} i\vec{\partial}_\perp \cdot \vec{A}_\perp + \frac{2g}{(i\partial^+)^2} \left\{ [i\partial^+ A_\perp^i, A_\perp^i] + 2\psi_+^\dagger T^a \psi_+ T^a \right\} \\ &\equiv \tilde{A}^- + \frac{2g}{(i\partial^+)^2} \left\{ [i\partial^+ A_\perp^i, A_\perp^i] + 2\psi_+^\dagger T^a \psi_+ T^a \right\} , \end{aligned} \quad (36)$$

with $\beta = \gamma^o$ and $\vec{\alpha}_\perp = \gamma^o \vec{\gamma}$.

To quantize, we expand the fields at $\tau = 0$ in terms of creation and annihilation operators,

$$\psi_+(x) = \int_{k^+ > 0} \frac{dk^+ d^2 k_\perp}{k^+ 16\pi^3} \sum_\lambda \left\{ b(\underline{k}, \lambda) u_+(\underline{k}, \lambda) e^{-ik \cdot x} \right.$$

$$\begin{aligned}
& + d^\dagger(\underline{k}, \lambda) v_+(\underline{k}, \lambda) e^{ik \cdot x} \} , \quad \tau = x^+ = 0 \\
A_\perp^i(x) &= \int_{k^+ > 0} \frac{dk^+ d^2 k_\perp}{k^+ 16\pi^3} \sum_\lambda \left\{ a(\underline{k}, \lambda) \epsilon_\perp^i(\lambda) e^{-ik \cdot x} + c \cdot c \right\} , \\
\tau &= x^+ = 0 , \tag{37}
\end{aligned}$$

with commutation relations ($\underline{k} = (k^+, \vec{k}_\perp)$):

$$\begin{aligned}
\{b(\underline{k}, \lambda), b^\dagger(\underline{p}, \lambda')\} &= \{d(\underline{k}, \lambda), d^\dagger(\underline{p}, \lambda')\} \\
&= [a(\underline{k}, \lambda), a^\dagger(\underline{p}, \lambda')] \\
&= 16\pi^3 k^+ \delta^3(\underline{k} - \underline{p}) \delta_{\lambda\lambda'} , \\
\{b, b\} = \{d, d\} &= \dots = 0 , \tag{38}
\end{aligned}$$

where λ is the quark or gluon helicity. These definitions imply canonical commutation relations for the fields with their conjugates ($\tau = x^+ = y^+ = 0, \underline{x} = (x^-, x_\perp), \dots$):

$$\begin{aligned}
\{\psi_+(\underline{x}), \psi_+^\dagger(\underline{y})\} &= \Lambda_+ \delta^3(\underline{x} - \underline{y}) , \\
[A^i(\underline{x}), \partial^+ A_\perp^j(\underline{y})] &= i\delta^{ij} \delta^3(\underline{x} - \underline{y}) . \tag{39}
\end{aligned}$$

The creation and annihilation operators define the Fock state basis for the theory at $\tau = 0$, with a vacuum $|0\rangle$ defined such that $b|0\rangle = d|0\rangle = a|0\rangle = 0$. The evolution of these states with τ is governed by the light-cone Hamiltonian, $H_{LC} = P^-$, conjugate to τ . The Hamiltonian can be readily expressed in terms of ψ_+ and A_\perp^i :

$$H_{LC} = H_0 + V , \tag{40}$$

where

$$\begin{aligned}
H_0 &= \int d^3x \left\{ \text{Tr} \left(\partial_\perp^i A_\perp^j \partial_\perp^i A_\perp^j \right) \right. \\
&+ \left. \psi_+^\dagger (i\partial_\perp \cdot \alpha_\perp + \beta m) \frac{1}{i\partial^+} (i\partial_\perp \cdot \alpha_\perp + \beta m) \psi_+ \right\} \\
&= \sum_\lambda \int \frac{dk^+ d^2 k_\perp}{16\pi^3 k^+} \left\{ a^\dagger(\underline{k}, \lambda) a(\underline{k}, \lambda) \frac{k_\perp^2}{k^+} + b^\dagger(\underline{k}, \lambda) b(\underline{k}, \lambda) \right. \\
&\times \left. \frac{k_\perp^2 + m^2}{k^+} + d^\dagger(\underline{k}, \lambda) b(\underline{k}, \lambda) \frac{k_\perp^2 + m^2}{k^+} \right\} + \text{constant} \tag{41}
\end{aligned}$$

is the free Hamiltonian and V the interaction:

$$V = \int d^3x \left\{ 2g \text{Tr} \left(i\partial^\mu \tilde{A}^\nu \left[\tilde{A}_\mu, \tilde{A}_\nu \right] \right) - \frac{g^2}{2} \text{Tr} \left(\left[\tilde{A}^\mu, \tilde{A}^\nu \right] \left[\tilde{A}_\mu, \tilde{A}_\nu \right] \right) \right\}$$

$$\begin{aligned}
& + g \bar{\psi} \tilde{A} \tilde{\psi} + g^2 \text{Tr} \left([i\partial^+ \tilde{A}^\mu, \tilde{A}_\mu] \frac{1}{(i\partial^+)^2} [i\partial^+ \tilde{A}^\nu, \tilde{A}_\nu] \right) \\
& + g^2 \bar{\psi} \tilde{A} \frac{\gamma^+}{2i\partial^+} \tilde{A} \tilde{\psi} - g^2 \bar{\psi} \gamma^+ \left(\frac{1}{(i\partial^+)^2} [i\partial^+ \tilde{A}^\nu, \tilde{A}_\nu] \right) \tilde{\psi} \\
& + \frac{g^2}{2} \bar{\psi} \gamma^+ T^a \psi \frac{1}{(i\partial^+)^2} \bar{\psi} \gamma^+ T^a \psi \left. \right\}, \tag{42}
\end{aligned}$$

with $\tilde{\psi} = \tilde{\psi}_- + \psi_+$ ($\rightarrow \psi$ as $g \rightarrow 0$) and $\tilde{A}^\mu = (0, \tilde{A}^-, A_\perp^i)$ ($\rightarrow A^\mu$ as $g \rightarrow 0$). The Fock states are obviously eigenstates of H_0 with

$$H_0 |n : k_i^+, k_{\perp i}\rangle = \sum_i \left(\frac{k_\perp^2 + m^2}{k^+} \right)_i |n : k_i^+, k_{\perp i}\rangle. \tag{43}$$

It is equally obvious that they are not eigenstates of V , though any matrix element of V between Fock states is trivially evaluated.

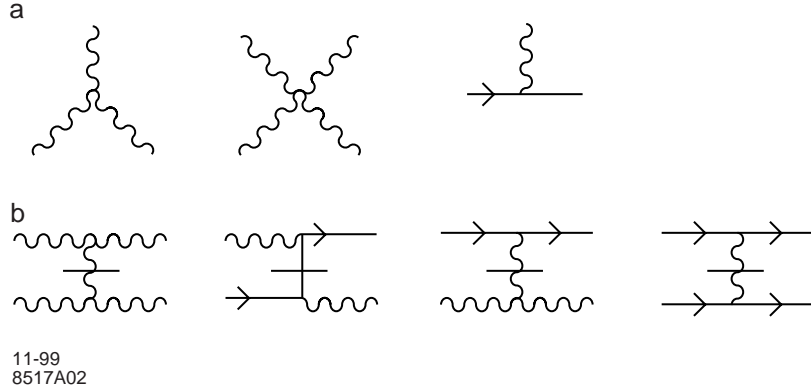


Figure 6: Diagrams which appear in the interaction Hamiltonian for QCD on the light cone. The propagators with horizontal bars represent “instantaneous” gluon and quark exchange which arise from reduction of the dependent fields in $A^+ = 0$ gauge. (a) Basic interaction vertices in QCD. (b) “Instantaneous” contributions.

The first three terms in V correspond to the familiar three and four gluon vertices, and the gluon-quark vertex [Fig. 6 (a)]. The remaining terms represent new four-quanta interactions containing instantaneous fermion and gluon propagators [Fig. 6 (b)]. All terms conserve total three-momentum $\underline{k} = (k^+, \vec{k}_\perp)$, because of the integral over \underline{x} in V . Furthermore, all Fock states other than the vacuum have total $k^+ >$

0, since each individual bare quantum has $k^+ > 0$. Consequently the Fock state vacuum must be an eigenstate of V and therefore an eigenstate of the full light-cone Hamiltonian.

Light-Cone Perturbation Theory

We define light-cone Green's functions to be the probability amplitudes that a state starting in Fock state $|i\rangle$ ends up in Fock state $|f\rangle$ a (light-cone) time τ later

$$\begin{aligned} \langle f|i\rangle G(f, i; \tau) &\equiv \langle f|e^{-iH_{LC}\tau/2}|i\rangle \\ &= i \int \frac{d\epsilon}{2\pi} e^{-i\epsilon\tau/2} G(f, i; \epsilon) \langle f|i\rangle, \end{aligned} \quad (44)$$

where Fourier transform $G(f, i; \epsilon)$ can be written

$$\begin{aligned} \langle f|i\rangle G(f, i; \epsilon) &= \left\langle f \left| \frac{1}{\epsilon - H_{LC} + i0_+} \right| i \right\rangle \\ &= \left\langle f \left| \frac{1}{\epsilon - H_{LC} + i0_+} + \frac{1}{\epsilon - H_0 + i0_+} V \frac{1}{\epsilon - H_0 + i0_+} \right. \right. \\ &\quad + \frac{1}{\epsilon - H_0 + i0_+} V \frac{1}{\epsilon - H_0 + i0_+} V \frac{1}{\epsilon - H_0 + i0_+} \\ &\quad \left. \left. + \dots \right| i \right\rangle. \end{aligned} \quad (45)$$

The rules for τ -ordered perturbation theory follow immediately when $(\epsilon - H_0)^{-1}$ is replaced by its spectral decomposition.

$$\frac{1}{\epsilon - H_0 + i0_+} = \sum_{n, \lambda_i} \int \tilde{\Pi} \frac{dk_i^+ d^2k_{\perp i}}{16\pi^3 k_i^+} \frac{|n : \underline{k}_i, \lambda_i\rangle \langle n : \underline{k}_i, \lambda_i|}{\epsilon - \sum_i (k^2 + m^2)_i / k_i^+ + i0_+} \quad (46)$$

The sum becomes a sum over all states n intermediate between two interactions.

To calculate $G(f, i; \epsilon)$ perturbatively then, all τ -ordered diagrams must be considered, the contribution from each graph computed according to the following rules:[153]

1. Assign a momentum k^μ to each line such that the total k^+, k_\perp are conserved at each vertex, and such that $k^2 = m^2$, *i.e.* $k^- = (k^2 + m^2)/k^+$. With fermions associate an on-shell spinor.

$$u(\underline{k}, \lambda) = \frac{1}{\sqrt{k^+}} \left(k^+ + \beta m + \vec{\alpha}_\perp \cdot \vec{k}_\perp \right) \begin{cases} \chi(\uparrow) & \lambda = \uparrow \\ \chi(\downarrow) & \lambda = \downarrow \end{cases} \quad (47)$$

or

$$v(\underline{k}, \lambda) = \frac{1}{\sqrt{k^+}} \left(k^+ - \beta m + \vec{\alpha}_\perp \cdot \vec{k}_\perp \right) \begin{cases} \chi(\downarrow) & \lambda = \uparrow \\ \chi(\uparrow) & \lambda = \downarrow \end{cases} \quad (48)$$

where $\chi(\uparrow) = 1/\sqrt{2}(1, 0, 1, 0)$ and $\chi(\downarrow) = 1/\sqrt{2}(0, 1, 0, -1)^T$. For gluon lines, assign a polarization vector $\epsilon^\mu = (0, 2\vec{\epsilon}_\perp \cdot \vec{k}_\perp/k^+, \vec{\epsilon}_\perp)$ where $\vec{\epsilon}_\perp(\uparrow) = -1/\sqrt{2}(1, i)$ and $\vec{\epsilon}_\perp(\downarrow) = 1/\sqrt{2}(1, -i)$.

2. Include a factor $\theta(k^+)/k^+$ for each internal line.
3. For each vertex include

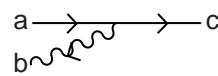

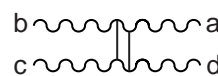
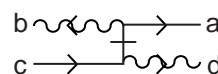
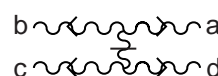
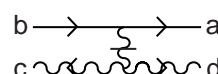
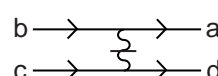
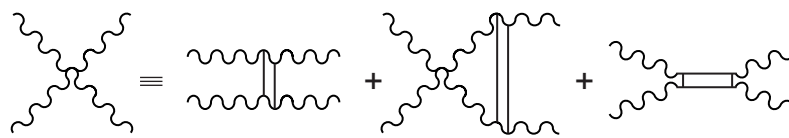
	<u>Vertex Factor</u>	<u>Color Factor</u>
	$g\bar{u}(c) \not{\epsilon}_b u(a)$	T^b
	$g\{(p_a - p_b) \cdot \epsilon_c^* \epsilon_a \cdot \epsilon_b$ + cyclic permutations}	iC^{abc}
	$g^2\{\epsilon_b \cdot \epsilon_c \epsilon_a^* \cdot \epsilon_d^* + \epsilon_a^* \cdot \epsilon_c \epsilon_b \cdot \epsilon_d^*\}$	$iC^{abe} iC^{cde}$
	$g^2 \bar{u}(a) \not{\epsilon}_b \frac{\gamma^+}{2(p_c^+ - p_d^+)} \not{\epsilon}_c^* u(c)$	$T^b T^d$
	$g^2 \epsilon_a^* \cdot \epsilon_b \frac{(p_a^+ - p_b^+)(p_c^+ - p_d^+)}{(p_c^+ + p_b^+)} \epsilon_d^* \cdot \epsilon_c$	$iC^{abe} iC^{cde}$
	$g^2 \bar{u}(a) \gamma^+ u(b) \frac{(p_c^+ - p_d^+)}{(p_c^+ + p_d^+)^2} \epsilon_d^* \cdot \epsilon_c$	$iC^{cde} T^e$
	$g^2 \frac{\bar{u}(a) \gamma^+ u(b) \bar{u}(d) \gamma^+ u(c)}{(p_c^+ - p_d^+)^2}$	$T^e T^e$
		
<small>11-99 8517A01</small>		

Figure 7: Graphical rules for QCD in light-cone perturbation theory.

factors as illustrated in Fig. 7. To convert incoming into outgoing lines or vice versa replace

$$u \leftrightarrow v, \quad \bar{u} \leftrightarrow -\bar{v}, \quad \epsilon \leftrightarrow \epsilon^* \quad (49)$$

in any of these vertices.

4. For each intermediate state there is a factor

$$\frac{1}{\epsilon - \sum_{\text{interm}} k^- + i0_+} \quad (50)$$

where ϵ is the incident P^- , and the sum is over all particles in the intermediate state.

5. Integrate $\int dk^+ d^2 k_\perp / 16\pi^3$ over each independent k , and sum over internal helicities and colors.
6. Include a factor -1 for each closed fermion loop, for each fermion line that both begins and ends in the initial state (*i.e.* $\bar{v} \dots u$), and for each diagram in which fermion lines are interchanged in either of the initial or final states.

As an illustration, the second diagram in Fig. 7 contributes

$$\begin{aligned} & \frac{1}{\epsilon - \sum_{i=b,d} \left(\frac{k_\perp^2 + m^2}{k^+} \right)_i} \cdot \frac{\theta(k_a^+ - k_b^+)}{k_a^+ - k_b^+} \\ & \times \frac{g^2 \sum_\lambda \bar{u}(b) \epsilon^*(\underline{k}_a - \underline{k}_b, \lambda) u(a) \bar{u}(d) \not{\epsilon}(\underline{k}_a - \underline{k}_b, \lambda) u(c)}{\epsilon - \sum_{i=b,c} \left(\frac{k_\perp^2 + m^2}{k^+} \right)_i - \frac{(k_{\perp a} - k_{\perp b})^2}{k_a^+ - k_b^+}} \\ & \cdot \frac{1}{\epsilon - \sum_{i=a,c} \left(\frac{k_\perp^2 + m^2}{k^+} \right)_i} \end{aligned} \quad (51)$$

(times a color factor) to the $q\bar{q} \rightarrow q\bar{q}$ Green's function. (The vertices for quarks and gluons of definite helicity have very simple expressions in terms of the momenta of the particles.) The same rules apply for scattering amplitudes, but with propagators omitted for external lines, and with $\epsilon = P^-$ of the initial (and final) states.

Finally, notice that this quantization procedure and perturbation theory (graph by graph) are manifestly invariant under a large class of Lorentz transformations:

1. boosts along the 3-direction—*i.e.* $p^+ \rightarrow K p^+$, $p^- \rightarrow K^{-1} p^-$, $p_\perp \rightarrow p_\perp$ for each momentum;

2. transverse boosts—*i.e.* $p^+ \rightarrow p^+$, $p^- \rightarrow p^- + 2p_\perp \cdot Q_\perp + p^+ Q_\perp^2$, $p_\perp \rightarrow p_\perp + p^+ Q_\perp$ for each momentum (Q_\perp like K is dimensionless);
3. rotations about the 3-direction.

It is these invariances which lead to the frame independence of the Fock state wave functions.

APPENDIX II

LIGHT CONE FOCK REPRESENTATION OF ELECTROWEAK CURRENTS

The light-cone Fock representation provides an explicit form for the matrix elements of electroweak currents $\langle A|J^\mu|B\rangle$ between hadrons B and A . The discussion in this appendix follows that of Ref. [35] The underlying formalism is the light-cone Hamiltonian Fock expansion in which hadron wavefunctions are decomposed on the free Fock basis of QCD. In this formalism, the full Heisenberg current J^μ can be equated to the current j^μ of the non-interacting theory which in turn has simple matrix elements on the free Fock basis.

Elastic form factors at space-like momentum transfer $q^2 = -Q^2 < 0$ are most simply evaluated from matrix elements of the “good” current $j^+ = j^0 + j^z$ in the preferred Lorentz frame where $q^+ = q^0 + q^z = 0$ [155, 156, 10]. The j^+ current has the advantage that it does not have large matrix elements to pair fluctuations, so that only diagonal, parton-number-conserving transitions need to be considered. The use of the j^+ current and the $q^+ = 0$ frame brings out striking advantage of the light-cone quantization formalism: only diagonal, parton-number-conserving Fock state matrix elements are required. However, in the case of the time-like form factors which occur in semileptonic heavy hadron decays, we need to choose a frame with $q^+ > 0$, where q^μ is the four-momentum of the lepton pair. Furthermore, in order to sort out the contributions to the various weak decay form factors, we need to evaluate the “bad” – current $j^- = j^0 - j^z$ as well as the “good” current j^+ . In such cases we will also require off-diagonal Fock state transitions; *i.e.* the convolution of Fock state wavefunctions differing by two quanta, a $q\bar{q}'$ pair. The entire electroweak current matrix element is then in general given by the sum of the diagonal $n \rightarrow n$

and off-diagonal $n + 1 \rightarrow n - 1$ transitions. As we shall see, an important feature of a general analysis is the emergence of singular $\delta(x)$ “zero-mode” contributions from the off-diagonal matrix elements if the choice of frame dictates $q^+ = 0$. The formulas [35] are in principle exact, given the light-cone wavefunctions of hadrons.

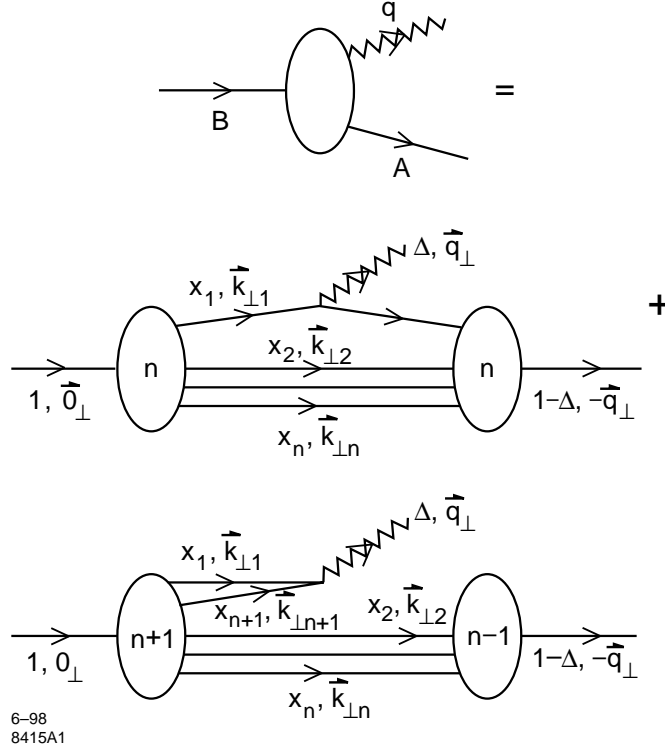


Figure 8: Exact representation of electroweak decays and time-like form factors in the light-cone Fock representation.

The evaluation of the timelike semileptonic decay amplitude $B \rightarrow A\ell\bar{\nu}$ requires the matrix element of the weak current between hadron states $\langle A|j^\mu(0)|B\rangle$. Here $x = \frac{k^+}{P^+} = \frac{k^0+k^3}{P^0+P^3}$ and we use the metric convention $a \cdot b = \frac{1}{2}(a^+b^- + a^-b^+) - \vec{a}_\perp \cdot \vec{b}_\perp$. (See Fig. 8.) The interaction current then has simple matrix elements of the free Fock amplitudes, with the proviso that all $x_i > 0$. We shall adopt the choice of a Lorentz general frame where the outgoing leptonic current carries $q^\mu = (q^+, q_\perp, q^-) = \left(\Delta P^+, q_\perp, \frac{q^2+q_\perp^2}{\Delta P^+}\right)$. The value of $\Delta = q^+/P^+$ is determined from four-momentum

conservation:

$$\frac{q^2 + q_\perp^2}{\Delta} + \frac{m_A^2 + q_\perp^2}{1 - \Delta} = m_B^2. \quad (52)$$

In the limit $\Delta \rightarrow 0$, the matrix element for the + vector current should coincide with the Drell-Yan West formula [155, 156, 10].

For the $n \rightarrow n$ diagonal term ($\Delta n = 0$), the final-state hadron wavefunction has arguments $\frac{x_1 - \Delta}{1 - \Delta}$, $\vec{k}'_{\perp 1} - \frac{1 - x_1}{1 - \Delta} \vec{q}_\perp$ for the struck quark and $\frac{x_i}{1 - \Delta}$, $\vec{k}'_{\perp i} + \frac{x_i}{1 - \Delta} \vec{q}_\perp$ for the $n - 1$ spectators. We thus have a formula for the diagonal (parton-number-conserving) matrix element of the form:

$$\begin{aligned} \langle A | J^\mu | B \rangle_{\Delta n = 0} &= \sum_{n, \lambda} \prod_{i=1}^n \int_\Delta^1 dx_1 \int_0^1 dx_{i(i \neq 1)} \int \frac{d^2 \vec{k}'_{\perp i}}{2(2\pi)^3} \\ &\times \delta \left(1 - \sum_{j=1}^n x_j \right) \delta^{(2)} \left(\sum_{j=1}^n \vec{k}'_{\perp j} \right) \\ &\times \psi_{A(n)}^\dagger(x'_i, \vec{k}'_{\perp i}, \lambda_i) j^\mu \psi_{B(n)}(x_i, \vec{k}_{\perp i}, \lambda_i), \end{aligned} \quad (53)$$

where

$$\begin{cases} x'_1 = \frac{x_1 - \Delta}{1 - \Delta}, & \vec{k}'_{\perp 1} = \vec{k}_{\perp 1} - \frac{1 - x_1}{1 - \Delta} \vec{q}_\perp & \text{for the struck quark} \\ x'_i = \frac{x_i}{1 - \Delta}, & \vec{k}'_{\perp i} = \vec{k}_{\perp i} + \frac{x_i}{1 - \Delta} \vec{q}_\perp & \text{for the } (n - 1) \text{ spectators.} \end{cases} \quad (54)$$

A sum over all possible helicities λ_i is understood. If quark masses are neglected the vector and axial currents conserve helicity. We also can check that $\sum_i^n x'_i = 1$, $\sum_i^n \vec{k}'_{\perp i} = \vec{0}_\perp$.

For the $n + 1 \rightarrow n - 1$ off-diagonal term ($\Delta n = -2$), let us consider the case where partons 1 and $n + 1$ of the initial wavefunction annihilate into the leptonic current leaving $n - 1$ spectators. Then $x_{n+1} = \Delta - x_1$, $\vec{k}'_{\perp n+1} = \vec{q}_\perp - \vec{k}_{\perp 1}$. The remaining $n - 1$ partons have total momentum $((1 - \Delta)P^+, -\vec{q}_\perp)$. The final wavefunction then has arguments $x'_i = \frac{x_i}{(1 - \Delta)}$ and $\vec{k}'_{\perp i} = \vec{k}_{\perp i} + \frac{x_i}{1 - \Delta} \vec{q}_\perp$. We thus obtain the formula for the off-diagonal matrix element:

$$\begin{aligned} \langle A | J^\mu | B \rangle_{\Delta n = -2} &= \sum_{n, \lambda} \int_0^\Delta dx_1 \int_0^1 dx_{n+1} \int \frac{d^2 \vec{k}'_{\perp 1}}{2(2\pi)^3} \int \frac{d^2 \vec{k}'_{\perp n+1}}{2(2\pi)^3} \\ &\times \prod_{i=2}^n \int_0^1 dx_i \int \frac{d^2 \vec{k}'_{\perp i}}{2(2\pi)^3} \delta \left(1 - \sum_{j=1}^{n+1} x_j \right) \delta^{(2)} \left(\sum_{j=1}^{n+1} \vec{k}'_{\perp j} \right) \end{aligned}$$

$$\begin{aligned}
& \times \psi_{A(n-1)}^\dagger(x'_i, \vec{k}'_{\perp i}, \lambda_i) j^\mu \psi_{B(n+1)} \\
& \times (\{x_1, x_i, x_{n+1} = \Delta - x_1\}, \\
& \times \{\vec{k}_{\perp 1}, \vec{k}_{\perp i}, \vec{k}_{\perp n+1} = \vec{q}_\perp - \vec{k}_{\perp 1}\}, \\
& \times \{\lambda_1, \lambda_i, \lambda_{n+1} = -\lambda_1\}).
\end{aligned} \tag{55}$$

Here $i = 2, 3, \dots, n$ with

$$x'_i = \frac{x_i}{1 - \Delta}, \quad \vec{k}'_{\perp i} = \vec{k}_{\perp i} + \frac{x_i}{1 - \Delta} \vec{q}_\perp \tag{56}$$

label the $n - 1$ spectator partons which appear in the final-state hadron wavefunction. We can again check that the arguments of the final-state wavefunction satisfy $\sum_{i=2}^n x'_i = 1$, $\sum_{i=2}^n \vec{k}'_{\perp i} = \vec{0}_\perp$. Similarly, in gauge theory with spin-half charged constituents, matrix elements of the “bad” currents J^\perp and J^- receive $\Delta n = \pm 1$ and $\Delta n = -3$ contributions from the induced instantaneous fermion exchange currents $q \rightarrow \gamma^* q q$, $g q \rightarrow \gamma^* q$, and $g q \bar{q} \rightarrow \gamma^*$. In the case of scalars, these contributions arise from the 4 point “seagull” interactions. Note that these terms do not occur for matrix elements of J^+ .

The free current matrix elements j^μ in the light-cone representation are easily constructed. For example, the vector current of quarks takes the form

$$j^\mu = \frac{\bar{u}(x', k'_\perp, \lambda') \gamma^\mu u(x, k_\perp, \lambda)}{\sqrt{k^+} \sqrt{k'^+}} \tag{57}$$

and

$$j^+ = 2\delta_{\lambda, \lambda'} . \tag{58}$$

The other light-cone spinor matrix elements of j^μ can be obtained from the tables in Ref. [11]. In the case of spin zero partons

$$j^+ = \frac{x + x'}{\sqrt{x x'}} \tag{59}$$

and

$$j^- = \frac{k^- + k'^-}{\sqrt{x x'} P^+}. \tag{60}$$

However, instead of evaluating each k^- in the j^- current from the on-shell condition $k^- k^+ = m^2$, one must instead evaluate the k^- of the struck partons from energy

conservation $k^- = p_{\text{initial}}^- - p_{\text{spectator}}^-$. This effect is seen explicitly when one integrates the covariant current over the denominator poles in the k^- variable. It can also be understood as due to the implicit inclusion of local instantaneous exchange contributions obtained in light-cone quantization [36, 157]. The mass $m_{\text{spectator}}^2$ which is needed for the evaluation of j^- current in the diagonal case is the mass of the entire spectator system. Thus $m_{\perp\text{spectator}}^2 = m_{\text{spectator}}^2 + \vec{k}_{\perp\text{spectator}}^2$, where $\vec{k}_{\perp\text{spectator}} = \sum_j \vec{k}_{\perp j}$ and $m_{\perp\text{spectator}}^2/x_{\text{spectator}} = \sum_j m_j^2/x_j$, summed over the j spectators. This is an important simplification for phenomenology, since we can change variables to $m_{\text{spectator}}^2$ and $d^2\vec{k}_{\perp\text{spectator}}$ and replace all of the spectators by a spectral integral over the cluster mass $m_{\text{spectator}}^2$.

The proper treatment of the J^- current implies consistency conditions which must be obeyed by the light-cone wavefunctions. For example, current conservation for the form factors of spin zero hadrons requires

$$(2p - q)^\mu F(q^2) = \langle p - q | J^\mu(0) | p \rangle \quad (61)$$

and thus

$$\langle p - q | J^+ | p \rangle = \frac{(2p - q)^+}{(2p - q)^-} \langle p - q | J^- | p \rangle . \quad (62)$$

We have explicitly verified this new type of virial theorem in a simple scalar composite model in Ref. [35].

The off-diagonal $n + 1 \rightarrow n - 1$ contributions provide a new perspective on the physics of B -decays. A semileptonic decay involves not only matrix element where a quark changes flavor, but also a contribution where the leptonic pair is created from the annihilation of a $q\bar{q}$ pair within the Fock states of the initial B wavefunction. The semileptonic decay thus can occur from the annihilation of a nonvalence quark-antiquark pair in the initial hadron. This feature will carry over to exclusive hadronic B -decays, such as $B^0 \rightarrow \pi^- D^+$. In this case the pion can be produced from the coalescence of a $d\bar{u}$ pair emerging from the initial higher particle number Fock wavefunction of the B . The D meson is then formed from the remaining quarks after the internal exchange of a W boson.

A remarkable advantage of the light-cone formalism that all matrix elements of local operators can be written down exactly in terms of simple convolutions of light-cone Fock wavefunctions. The light-cone wavefunctions depend only on the hadron itself;

they are process-independent. The formalism is relativistic and frame-independent—the incident four-vectors can be chosen in any frame. Note that the matrix element of a current in the covariant Bethe-Salpeter formalism requires the construction of the current from insertions into an infinite number of irreducible kernels. The Bethe-Salpeter formalism becomes even more intractable for bound-states of more than two particles.

APPENDIX III BARYON FORM FACTORS AND EVOLUTION EQUATIONS

The baryon form factor is a prototype for the calculation of the QCD hard scattering contribution for the whole range of exclusive processes at large momentum transfer. Away from possible special points in the x_i integrations a general hadronic amplitude can be written to leading order in $1/Q^2$ as a convolution of a connected hard-scattering amplitude T_H convoluted with the meson and baryon distribution amplitudes:

$$\phi_M(x, Q) = \int^{|\mathcal{E}| < Q^2} \frac{d^2 k_\perp}{16\pi^2} \psi_{q\bar{q}}^Q(x, \vec{k}_\perp) \quad , \quad (63)$$

and

$$\phi_B(x_i, Q) = \int^{|\mathcal{E}| < Q^2} [d^2 k_\perp] \psi_{qqq}(x_i, \vec{k}_{\perp i}) \quad . \quad (64)$$

Here $\mathcal{E} = \mathcal{M}_{qqq}^2 - M_B^2$ is the invariant off-shellness of the three-quark baryon light-cone wavefunction.

The hard scattering amplitude T_H is computed by replacing each external hadron line by massless valence quarks each collinear with the hadron's momentum $p_i^\mu \cong x_i p_H^\mu$. For example the baryon form factor at large Q^2 has the form [153, 158]

$$G_M(Q^2) = \int [dx][dy] \phi^*(y_i, \bar{Q}) T_H(x, y; Q^2) \phi(x, \bar{Q}) \quad (65)$$

where T_H is the $3q + \gamma \rightarrow 3q'$ amplitude. For the proton and neutron we have to leading order [$C_B = 2/3$]

$$\begin{aligned} T_p &= \frac{128\pi^2 C_B^2}{(Q^2 + M_0^2)^2} T_1 \\ T_n &= \frac{128\pi^2 C_B^2}{3(Q^2 + M_0^2)^2} [T_1 - T_2] \end{aligned} \quad (66)$$

where

$$\begin{aligned}
T_1 = & - \frac{\alpha_s(x_3 y_3 Q^2) \alpha_s(1-x_1)(1-y_1)Q^2}{x_3(1-x_1)^2 y_3(1-y_1)^2} \\
& + \frac{\alpha_s(x_2 y_2 Q^2) \alpha_s((1-x_1)(1-y_1)Q^2)}{x_2(1-x_1)^2 y_2(1-y_1)^2} \\
& - \frac{\alpha_s(x_2 y_2 Q^2) \alpha_s(x_3 y_3 Q^2)}{x_2 x_3(1-x_3) y_2 y_3(1-y_1)} ,
\end{aligned} \tag{67}$$

and

$$T_2 = - \frac{\alpha_s(x_1 y_1 Q^2) \alpha_s(x_3 y_3 Q^2)}{x_1 x_3(1-x_1) y_1 y_3(1-y_3)} . \tag{68}$$

T_1 corresponds to the amplitude where the photon interacts with the quarks (1) and (2) which have helicity parallel to the nucleon helicity, and T_2 corresponds to the amplitude where the quark with opposite helicity is struck. The running coupling constants have arguments \hat{Q}^2 corresponding to the gluon momentum transfer of each diagram. Only the large Q^2 behavior is predicted by the theory; we utilize the parameter M_0 to represent the effect of power-law suppressed terms from mass insertions, higher Fock states, etc.

The Q^2 -evolution of the baryon distribution amplitude can be derived from the operator product expansion of three quark fields or from the gluon exchange kernel. The baryon evolution equation to leading order in α_s is [158]

$$x_1 x_2 x_3 \left\{ \frac{\partial}{\partial \zeta} \tilde{\phi}(x_i, Q) + \frac{3}{2} \frac{C_F}{\beta_0} \tilde{\phi}(x_i, Q) \right\} = \frac{C_B}{\beta_0} \int_0^1 [dy] V(x_i, y_i) \tilde{\phi}(y_i, Q). \tag{69}$$

Here $\phi = x_1 x_2 x_3 \tilde{\phi}$, $\zeta = \log(\log Q^2 / \Lambda^2)$, $C_F = (n_c^2 - 1)/2n_c = 4/3$, $C_B = (n_c + 1)/2n_c = 2/3$, $\beta = 11 - (2/3)n_f$, and $V(x_i, y_i)$ is computed to leading order in α_s from the single-gluon-exchange kernel:

$$\begin{aligned}
V(x_i, y_i) &= 2x_i x_2 x_3 \sum_{i \neq j} \theta(y_i - x_i) \delta(x_k - y_k) \frac{y_j}{x_j} \left(\frac{\delta_{h_i \bar{h}_j}}{x_i + x_j} + \frac{\Delta}{y_i - x_i} \right) \\
&= V(y_i, x_i) .
\end{aligned} \tag{70}$$

The infrared singularity at $x_i = y_i$ is cancelled because the baryon is a color singlet.

The baryon evolution equation automatically sums to leading order in $\alpha_s(Q^2)$ all of the contributions from multiple gluon exchange which determine the tail of the valence wavefunction and thus the Q^2 -dependence of the distribution amplitude. The

general solution of this equation is

$$\phi(x_i, Q) = x_1 x_2 x_3 \sum_{n=0}^{\infty} a_n \left(\ell n \frac{Q^2}{\Lambda^2} \right)^{-\gamma_n} \phi_n(x_i) \quad , \quad (71)$$

where the anomalous dimensions γ_n and the eigenfunctions $\tilde{\phi}_n(x_i)$ satisfy the characteristic equation:

$$x_1 x_2 x_3 \left(-\gamma_n + \frac{3C_F}{2\beta} \right) \tilde{\phi}_n(x_i) = \frac{C_B}{\beta} \int_0^1 [dy] V(x_i, y_i) \tilde{\phi}_n(y_i) \quad . \quad (72)$$

A useful technique for obtaining the solution to evolution equations is to construct completely antisymmetric representations as a polynomial orthonormal basis for the distribution amplitude of multi-quark bound states. In this way one obtain a distinctive classification of nucleon (N) and delta (Δ) wave functions and the corresponding Q^2 dependence which discriminates N and Δ form factors. This technique is developed in detail in Ref. [159]. The conformal representation of baryon distribution amplitudes is given in Ref. [70].

Taking into account the evolution of the baryon distribution amplitude, the nucleon magnetic form factors at large Q^2 , has the form [153, 158]

$$G_M(Q^2) \rightarrow \frac{\alpha_s^2(Q^2)}{Q^4} \sum_{n,m} b_{nm} \left(\log \frac{Q^2}{\Lambda^2} \right)^{\gamma_n^B - \gamma_m^B} \left[1 + \mathcal{O} \left(\alpha_s(Q^2), \frac{m^2}{Q^2} \right) \right] \quad . \quad (73)$$

where the γ_n are computable anomalous dimensions of the baryon three-quark wave function at short distance and the b_{mn} are determined from the value of the distribution amplitude $\phi_B(x, Q_0^2)$ at a given point Q_0^2 and the normalization of T_H . Asymptotically, the dominant term has the minimum anomalous dimension. The dominant part of the form factor comes from the region of the x_i integration where each quark has a finite fraction of the light cone momentum. The integrations over x_i and y_i have potential endpoint singularities. However, it is easily seen that any anomalous contribution [*e.g.* from the region $x_2, x_3 \sim \mathcal{O}(m/Q)$, $x_1 \sim 1 - \mathcal{O}(m/Q)$] is asymptotically suppressed at large Q^2 by a Sudakov form factor arising from the virtual correction to the $\bar{q}\gamma q$ vertex when the quark legs are near-on-shell [$p^2 \sim \mathcal{O}(mQ)$] [158, 160]. This Sudakov suppression of the endpoint region requires an all orders resummation of perturbative contributions, and thus the derivation of the baryon form factors is not as rigorous as for the meson form factor, which has no such endpoint singularity [160].

One can also use PQCD to predict ratios of various baryon and isobar form factors assuming isospin or $SU(3)$ -flavor symmetry for the basic wave function structure. Results for the neutral weak and charged weak form factors assuming standard $SU(2) \times U(1)$ symmetry are given in Ref. [161].

Comparison Between Time-Ordered and τ -Ordered Perturbation Theory

Equal t	Equal $\tau = t + z$
$k^o = \sqrt{\vec{k}^2 + m^2}$ (particle mass shell)	$k^- = \frac{k_\perp^2 + m^2}{k^+}$ (particle mass shell)
$\Sigma \vec{k}$ conserved	$\Sigma \vec{k}_\perp, k^+$ conserved
$\mathcal{M}_{ab} = V_{ab} + \sum_c V_{ac} \frac{1}{\sum_a k^o - \sum_c k^o + i\epsilon} V_{cb}$	$\mathcal{M}_{ab} = V_{ab} + \sum_c V_{ac} \frac{1}{\sum_a k^- - \sum_c k^- + i\epsilon} V_{cb}$
$n!$ time-ordered contributions	$k^+ > 0$ only
Fock states $\psi_n(\vec{k}_i)$	Fock states $\psi_n(\vec{k}_{\perp i}, x_i)$
$\sum_{i=1}^n \vec{k}_i = \vec{P} = 0$	$x = \frac{k^+}{P^+}, \sum_{i=1}^n x_i = 1, \sum_{i=1}^n \vec{k}_{\perp i} = 0$ ($0 < x_i < 1$)
$\mathcal{E} = P^o - \sum_{i=1}^n k_i^o$ $= M - \sum_{i=1}^n \sqrt{k_i^2 + m_i^2}$	$\mathcal{E} = P^+ \left(P^- - \sum_{i=1}^n k_i^- \right)$ $= M^2 - \sum_{i=1}^n \left(\frac{k_\perp^2 + m^2}{x} \right)_i$

References

- [1] J.D. Bjorken, *Phys. Rev.* **148**, 1467 (1966).
- [2] M. Breidenbach *et al.*, *Phys. Rev. Lett.* **23**, 935 (1969).
- [3] J. P. Nasalski [New Muon Collaboration], *Nucl. Phys.* **A577**, 325C (1994).
- [4] V. Barone, C. Pascaud and F. Zomer, hep-ph/9907512.
- [5] M. Karliner and H. J. Lipkin, hep-ph/9906321.
- [6] S. J. Brodsky, P. Hoyer, C. Peterson, and N. Sakai, *Phys. Lett.* **93B**, 451 (1980).
- [7] B. W. Harris, J. Smith and R. Vogt, *Nucl. Phys.* **B461**, 181 (1996) hep-ph/9508403.
- [8] S. J. Brodsky, H. Pauli and S. S. Pinsky, *Phys. Rept.* **301**, 299 (1998), hep-ph/9705477.
- [9] S. J. Brodsky and A. H. Mueller, *Phys. Lett.* **206B**, 685 (1988). L. Frankfurt and M. Strikman, *Phys. Rept.* **160**, 235 (1988); P. Jain, B. Pire and J. P. Ralston, *Phys. Rept.* **271**, 67 (1996).
- [10] S. J. Brodsky and S. D. Drell, *Phys. Rev.* **D22**, 2236 (1980).
- [11] G. P. Lepage and S. J. Brodsky, *Phys. Rev.* **D22**, 2157 (1980); *Phys. Lett.* **B87**, 359 (1979); *Phys. Rev. Lett.* **43**, 545, 1625(E) (1979).
- [12] S.D. Bass, S.J. Brodsky and I. Schmidt, *Phys. Rev.* **D60**, 034010 (1999) hep-ph/9901244.
- [13] A. Szczepaniak, E. M. Henley and S. J. Brodsky, *Phys. Lett.* **B243**, 287 (1990).
- [14] M. Beneke, G. Buchalla, M. Neubert and C. T. Sachrajda, hep-ph/9905312.
- [15] A. Szczepaniak, *Phys. Rev.* **D54**, 1167 (1996).
- [16] P. Ball and V. M. Braun, *Phys. Rev.* **D58**, 094016 (1998) hep-ph/9805422.

- [17] H. C. Pauli and S. J. Brodsky, *Phys. Rev.* **D32**, 1993 (1985); *Phys. Rev.* **D32**, 2001 (1985).
- [18] S. Dalley, and I. R. Klebanov, *Phys. Rev.* **D47**, 2517 (1993).
- [19] F. Antonuccio and S. Dalley, *Phys. Lett.* **B348**, 55 (1995); *Phys. Lett.* **B376**, 154 (1996); *Nucl. Phys.* **B461**, 275 (1996).
- [20] F. Antonuccio, I. Filippov, P. Haney, O. Lunin, S. Pinsky, U. Trittman and J. Hiller [SDLCQ Collaboration], hep-th/9910012.
- [21] P. P. Srivastava and S. J. Brodsky, hep-ph/9906423.
- [22] S. J. Brodsky, Y. Frishman, G. P. Lepage and C. Sachrajda, *Phys. Lett.* **91B**, 239 (1980).
- [23] D. Müller, *Phys. Rev.* **D49**, 2525 (1994).
- [24] S. J. Brodsky and H. J. Lu, *Phys. Rev.* **D51**, 3652 (1995) hep-ph/9405218.
- [25] S. J. Brodsky, G. T. Gabadadze, A. L. Kataev and H. J. Lu, *Phys. Lett.* **B372**, 133 (1996) hep-ph/9512367.
- [26] S. J. Brodsky and J. Rathsman, hep-ph/9906339.
- [27] S. J. Brodsky, E. Gardi, G. Grunberg, and J. Rathsman, in progress.
- [28] S. J. Brodsky and P. Huet, *Phys. Lett.* **B417**, 145 (1998) hep-ph/9707543.
- [29] S. J. Brodsky and H. C. Pauli, *lectures given at 30th Schladming Winter School in Particle Physics: Field Theory, Schladming, Austria, Feb 27 - Mar 8, 1991.*
- [30] S. J. Brodsky, J. R. Hiller and G. McCartor, *Phys. Rev.* **D58**, 025005 (1998) hep-th/9802120.
- [31] S. J. Brodsky, G. P. Lepage and P. B. Mackenzie, *Phys. Rev.* **D28**, 228 (1983).
- [32] S. J. Brodsky, C.-R. Ji, A. Peng and D. G. Robertson, *Phys. Rev.* **D57**, 345 (1998).
- [33] N. J. Watson, *Nucl. Phys.* **B494**, 388 (1997) hep-ph/9606381.

- [34] A. Czarnecki, K. Melnikov and N. Uraltsev, *Phys. Rev. Lett.* **80**, 3189 (1998) hep-ph/9708372.
- [35] S. J. Brodsky and D. S. Hwang, *Nucl. Phys.* **B543**, 239 (1999) hep-ph/9806358.
- [36] S. J. Chang, R. G. Root and T. M. Yan, *Phys. Rev.* **D7**, 1133 (1973).
- [37] M. Burkardt, *Nucl. Phys.* **A504**, 762 (1989); *Nucl. Phys.* **B373**, 613 (1992); *Phys. Rev.* **D52**, 3841 (1995).
- [38] H. Choi and C. Ji, *Phys. Rev.* **D58**, 071901 (1998) hep-ph/9805438.
- [39] K. Hornbostel, S. J. Brodsky, and H. C. Pauli, *Phys. Rev.* **D41** 3814 (1990).
- [40] P. Ball, *JHEP* **09**, 005 (1998), hep-ph/9802394.
- [41] S. J. Brodsky and G. P. Lepage, in *Perturbative Quantum Chromodynamics*, A. H. Mueller, Ed. (World Scientific, 1989).
- [42] S. J. Brodsky, L. Frankfurt, J. F. Gunion, A. H. Mueller, and M. Strikman, *Phys. Rev.* **D50**, 3134 (1994), hep-ph/9402283.
- [43] F. Antonuccio, S. J. Brodsky, and S. Dalley, *Phys. Lett.* **B412** 104 (1997), hep-ph/9705413.
- [44] A. H. Mueller, *Phys. Lett.* **B308**, 355 (1993).
- [45] D. Mueller, SLAC-PUB-6496, May 1994, hep-ph/9406260.
- [46] S. J. Brodsky and I. A. Schmidt, *Phys. Lett.* **B234**, 144 (1990).
- [47] S. J. Brodsky, P. Hoyer, A. H. Mueller, W.-K. Tang, *Nucl. Phys.* **B369**, 519 (1992).
- [48] S. J. Brodsky and M. Karliner, *Phys. Rev. Lett.* **78**, 4682 (1997) hep-ph/9704379.
- [49] M. Burkardt and Brian Warr, *Phys. Rev.* **D45**, 958 (1992).
- [50] A. I. Signal and A. W. Thomas, *Phys. Lett.* **191B**, 205 (1987).
- [51] S. J. Brodsky and B.-Q. Ma, *Phys. Lett.* **B381**, 317 (1996), hep-ph/9604393.

- [52] See Ref. [9]. R. Vogt, S. J. Brodsky, and P. Hoyer, *Nucl. Phys.* **B360**, 67 (1991); *Nucl. Phys.* **B383**, 643 (1992).
- [53] P. Hoyer and S. Peigne, *Phys. Rev.* **D59**, 034011 (1999) hep-ph/9806424.
- [54] E. L. Berger and S. J. Brodsky, *Phys. Rev. Lett.* **42**, 940 (1979).
- [55] A. Brandenburg, S. J. Brodsky, V.V. Khoze, and D. Mueller, *Phys. Rev. Lett.* **73**, 939 (1994), hep-ph/9403361.
- [56] S. J. Brodsky and B. T. Chertok, *Phys. Rev.* **D14**, 3003 (1976).
- [57] S. J. Brodsky, C.-R. Ji, and G. P. Lepage, *Phys. Rev. Lett.* **51**, 83 (1983).
- [58] G. R. Farrar, K. Huleihel and H. Zhang, *Phys. Rev. Lett.* **74**, 650 (1995).
- [59] A. D. Krisch, *Nucl. Phys. B (Proc. Suppl.)* **25**, 285 (1992).
- [60] S. J. Brodsky and G. F. de Teramond, *Phys. Rev. Lett.* **60**, 1924 (1988).
- [61] S. J. Brodsky, C. Ji, A. Pang and D. G. Robertson, *Phys. Rev.* **D57**, 245 (1998) hep-ph/9705221.
- [62] S. J. Brodsky and G. R. Farrar, *Phys. Rev.* **D11**, 1309 (1975).
- [63] V. A. Matveev, R. M. Muradian and A. N. Tavkhelidze, *Nuovo Cim. Lett.* **7**, 719 (1973).
- [64] P.V. Landshoff, *Phys. Rev.* **D10**, 1024 (1974).
- [65] S. J. Brodsky and G. P. Lepage, *Phys. Rev.* **D24**, 2848 (1981).
- [66] V. Chernyak, hep-ph/9906387.
- [67] L. Frankfurt, G. A. Miller and M. Strikman, *Comments Nucl. Part. Phys.* **21**, 1 (1992).
- [68] M. R. Adams *et al.* [E665 Collaboration], *Z. Phys.* **C74**, 237 (1997).
- [69] P. Ball and V. M. Braun, *Nucl. Phys.* **B543**, 201 (1999) hep-ph/9810475.

- [70] V. M. Braun, S. E. Derkachov, G. P. Korchemsky and A. N. Manashov, hep-ph/9902375.
- [71] J. C. Collins, L. Frankfurt and M. Strikman, hep-ph/9709336.
- [72] C. E. Carlson and A. B. Wakely, *Phys. Rev.* **D48**, 2000 (1993); A. Afanasev, C. E. Carlson and C. Wahlquist, *Phys. Lett.* **B398**, 393 (1997), hep-ph/9701215, and *Phys. Rev.* **D58**, 054007 (1998), hep-ph/9706522.
- [73] S. J. Brodsky, M. Diehl, P. Hoyer and S. Peigne, *Phys. Lett.* **B449**, 306 (1999) hep-ph/9812277.
- [74] J. F. Gunion, S. J. Brodsky and R. Blankenbecler, *Phys. Rev.* **D6**, 2652 (1972); R. Blankenbecler and S. J. Brodsky, *Phys. Rev.* **D10**, 2973 (1974).
- [75] J. Gronberg *et al.* [CLEO Collaboration], *Phys. Rev.* **D57**, 33 (1998) hep-ex/9707031.
- [76] D. F. Ashery *et al.*, Fermilab E791 Collaboration, to be published.
- [77] S. J. Brodsky, Y. Frishman and G. P. Lepage, *Phys. Lett.* **167B**, 347 (1986).
- [78] J. C. Collins, L. Frankfurt and M. Strikman, *Phys. Rev.* **D56**, 2982 (1997) hep-ph/9611433.
- [79] G. Bertsch, S. J. Brodsky, A. S. Goldhaber, and J. F. Gunion, *Phys. Rev. Lett.* **47**, 297 (1981).
- [80] L. Frankfurt, G. A. Miller, and M. Strikman, *Phys. Lett.* **B304**, 1 (1993), hep-ph/9305228.
- [81] L. Frankfurt, G. A. Miller and M. Strikman, hep-ph/9907214.
- [82] P. Kroll and M. Raulfs, *Phys. Lett.* **B387**, 848 (1996).
- [83] I. V. Musatov and A. V. Radyushkin, *Phys. Rev.* **D56**, 2713 (1997).
- [84] T. Feldmann, hep-ph/9907226.
- [85] A. Schmedding and O. Yakovlev, hep-ph/9905392.

- [86] P. Stoler, *Few Body Syst. Suppl.* **11**, 124 (1999).
- [87] B. Melic, B. Nizic and K. Passek, hep-ph/9903426.
- [88] A. Szczepaniak, A. Radyushkin and C. Ji, *Phys. Rev.* **D57**, 2813 (1998) hep-ph/9708237.
- [89] C. J. Bebek *et al.*, *Phys. Rev.* **D13**, 25 (1976).
- [90] R. J. Holt, *Phys. Rev.* **C41**, 2400 (1990).
- [91] C. Bochna *et al.* [E89-012 Collaboration], *Phys. Rev. Lett.* **81**, 4576 (1998) nucl-ex/9808001.
- [92] M. K. Jones *et al.* [Jefferson Lab Hall A Collaboration], nucl-ex/9910005.
- [93] M. Ambrogiani *et al.* [E835 Collaboration], FERMILAB-PUB-99-027-E.
- [94] N. Isgur and C. H. Llewellyn Smith, *Phys. Lett.* **B217**, 535 (1989).
- [95] A. V. Radyushkin, *Phys. Rev.* **D58**, 114008 (1998) hep-ph/9803316.
- [96] J. Bolz and P. Kroll, *Z. Phys.* **A356**, 327 (1996) hep-ph/9603289.
- [97] A. S. Kronfeld and B. Nizic, *Phys. Rev.* **D44**, 3445 (1991).
- [98] S. J. Brodsky, F. E. Close and J. F. Gunion, *Phys. Rev.* **D6**, 177 (1972).
- [99] For reviews and further references see S. J. Brodsky and G. P. Lepage, SLAC-PUB-4947. Published in 'Perturbative Quantum Chromodynamics', Ed. by A.H. Mueller, World Scientific Publ. Co. (1989), p. 93-240 (QCD161:M83); V. L. Chernyak and A. R. Zhitnitsky, *Phys. Rept.* **112**, 173 (1984).
- [100] S. J. Brodsky, P. Hoyer, and S. Peigne, in preparation.
- [101] X. Ji, *Phys. Rev.* **D55**, 7114 (1997), hep-ph/9609381; X. Ji and J. Osborne, *Phys. Rev.* **D58**, 094018 (1998), hep-ph/9801260; A.V. Radyushkin, *Phys. Rev.* **D56**, 5524 (1997), hep-ph/9704207.
- [102] G. Grunberg, *Phys. Lett.* **B85**, 70 (1980); *Phys. Lett.* **B110**, 501 (1982); *Phys. Rev.* **D29**, 2315 (1984).

- [103] A. Dhar and V. Gupta, Phys. Rev. **D29**, 2822 (1984).
- [104] V. Gupta, D. V. Shirkov and O. V. Tarasov, Int. J. Mod. Phys. **A6**, 3381 (1991).
- [105] See Ref. [34] and Yu. L. Dokshitzer and B. R. Webber, Phys. Lett. **B404**, 321 (1997).
- [106] S. Adler, Phys. Rev. **182**, 1517 (1969).
- [107] A. C. Mattingly and P. M. Stevenson, Phys. Rev. **D49**, 437 (1994).
- [108] CCFR Collaboration, W.C. Leung, *et al.*, Phys. Lett. **B317**, 655 (1993).
- [109] CCFR and NuTeV Collaboration, presented by D. Harris at XXX Recontre de Moriond, 1995, presented by J. H. Kim at the European Conference on High Energy Physics, Brussels, July 1995.
- [110] A. L. Kataev, A.V. Sidorov, Phys. Lett. **B331**, 179 (1994).
- [111] CCFR Collaboration, P. Z. Quinta, *et al.*, Phys. Rev. Lett. **71**, 1307 (1993).
- [112] G. 't Hooft, in the Proceedings of the International School, Erice, Italy, 1977, edited by A. Zichichi, Subnuclear Series Vol. 15 (Plenum, New York, 1979).
- [113] H. J. Lu, Phys. Rev. **D45**, 1217 (1992)..
- [114] M. Beneke and V. M. Braun, Phys. Lett. **B348**, 513 (1995).
- [115] G. Peter Lepage and P. B. Mackenzie, Phys. Rev. **D48**, 2250 (1993).
- [116] M. Neubert, Phys. Rev. **D51**, 5924 (1995).
- [117] P. Ball, M. Beneke and V. M. Braun, Nucl. Phys. **B452**, 563 (1995).
- [118] A. De Rújula and H. Georgi, Phys. Rev. **D13**, 1296 (1976).
- [119] H. Georgi and H. D. Politzer, Phys. Rev. **D14**, 1829 (1976).
- [120] D. V. Shirkov, Teor. Mat. Fiz. **98**, 500 (1992) [Theor. Math. Phys. **93**, 1403 (1992)]; D. V. Shirkov and S. V. Mikhailov, Zeit. Phys. **C63**, 463 (1994).
- [121] J. Chýla, Phys. Lett. **B 351**, 325 (1995).

- [122] T. Appelquist, J. Carazzone, Phys. Rev. **D11**, 2856 (1975).
- [123] M. Melles, hep-ph/9805216, Phys. Rev. **D58**, 114004, 1998.
- [124] G. P. Lepage, J. Comp. Phys. **27**, 192 (1978); G. P. Lepage, Cornell preprint, CLNS-80/447, March 1980.
- [125] M. Peter, Nucl. Phys. **B501**, 471 (1997).
- [126] S. J. Brodsky, M. S. Gill, M. Melles, and J. Rathsman, Phys. Rev. **D58**, 116006 (1998).
- [127] T. Yoshino, K. Hagiwara, Z. Phys. **C 24**, 185 (1984).
- [128] F. Jegerlehner, O.V. Tarasov, hep-ph/9809485 and DESY 98-093.
- [129] C.T.H. Davies, *et al.*, Phys. Lett. **B345**, 42 (1995); Phys. Rev. **D56**, 2755 (1997).
- [130] B. H. Smith, M. B. Voloshin, Phys. Lett. **B324**, 117 (1994). Erratum-ibid. **B333**, 564 (1994).
- [131] S. J. Brodsky, A. H. Hoang, J. H. Kuhn, and T. Teubner, Phys. Lett. **B359**, 355 (1995).
- [132] V. S. Fadin, V. A. Khoze, A. D. Martin, and W. J. Stirling, Phys. Lett. **B363**, 112 (1995).
- [133] P. N. Burrows, Acta Phys. Polon. **B28**, 701 (1997).
- [134] S. J. Brodsky, P. Damgaard, Y. Frishman and G. P. Lepage, Phys. Rev. **D33**, 1881 (1986).
- [135] D. Muller, Phys. Rev. **D59**, 116001 (1999); A. V. Belitsky and D. Muller, Nucl. Phys. **B537**, 397 (1999); and Ref. [23].
- [136] J. Blumlein, V. Ravindran and W. L. van Neerven, hep-ph/9812450.

- [137] V. S. Fadin, E. A. Kuraev and L. N. Lipatov, Phys. Lett. **60B**, 50 (1975); L. N. Lipatov, Yad. Fiz. **23**, 642 (1976) [Sov. J. Nucl. Phys. **23**, 338 (1976)]; E. A. Kuraev, L. N. Lipatov and V. S. Fadin, Zh. Eksp. Teor. Fiz. **71**, 840 (1976) [Sov. JETP **44**, 443 (1976)]; *ibid.* **72**, 377 (1977) [**45**, 199 (1977)]; Ya. Ya. Balitskii and L. N. Lipatov, Yad. Fiz. **28**, 1597 (1978) [Sov. J. Nucl. Phys. **28**, 822 (1978)].
- [138] V. S. Fadin and L. N. Lipatov, Phys. Lett. **429B**, 127 (1998).
- [139] G. Camici and M. Ciafaloni, Phys. Lett. **430B**, 349 (1998).
- [140] W. A. Bardeen, A. J. Buras, D. W. Duke and T. Muta, Phys. Rev. **D18**, 3998 (1978).
- [141] S. J. Brodsky, V. S. Fadin, V.T. Kim, L. N. Lipatov and G. B. Pivovarov, hep-ph/9901229.
- [142] W. Celmaster and R. J. Gonsalves, Phys. Rev. **D20**, 1420 (1979); Phys. Rev. Lett. **42**, 1435 (1979).
- [143] P. Pascual and R. Tarrach, Nucl. Phys. **B174**, 123 (1980); (E) **B181**, 546 (1981).
- [144] W. Celmaster and P. M. Stevenson, Phys. Lett. **125B**, 493 (1983).
- [145] L. N. Lipatov, Phys. Rept. **C286**, 131 (1997).
- [146] L. N. Lipatov, Zh. Eksp. Teor. Fiz. **90**, 1536 (1986) [Sov. JETP **63**, 904 (1986)]; in *Perturbative Quantum Chromodynamics*, ed. A.H. Mueller (World Scientific, Singapore, 1989) p. 411; R. Kirschner and L. Lipatov, Zeit. Phys. **C45**, 477 (1990).
- [147] S. J. Brodsky, F. Hautmann and D.E. Soper, Phys. Rev. **D56**, 6957 (1997); S. J. Brodsky, F. Hautmann and D. E. Soper, Phys. Rev. Lett. **78**, 803 (1997); F. Hautmann, talk at ICHEP96 (Warsaw, July 1996), preprint OITS 613/96, in Proceedings of the XXVIII International Conference on High Energy Physics, eds. Z. Ajduk and A. K. Wroblewski, World Scientific, p.705; J. Bartels, A. De Roeck and H. Lotter, Phys. Lett. **B389**, 742 (1996).

- [148] S. J. Brodsky, E. Gardi, G. Grunberg, and J. Rathsman (in preparation).
- [149] S. J. Brodsky, J. R. Pelaez and N. Toumbas, Phys. Rev. **D60**, 037501 (1999)
hep-ph/9810424.
- [150] I. I. Balitsky and L. N. Lipatov, Sov. J. Nucl. Phys. **28**, 822 (1978).
- [151] S. J. Brodsky, F. Hautmann and D. E. Soper, Phys. Rev. **D56**, 6957 (1997)
hep-ph/9706427.
- [152] P.J. Mulders and M. Boggione, hep-ph/9907356.
- [153] G. P. Lepage and S. J. Brodsky, Phys. Rev. **D22**, 2157 (1980); Phys. Lett. **87B**,
359 (1979); Phys. Rev. Lett. **43**, 545, 1625(E) (1979).
- [154] G. P. Lepage, S. J. Brodsky, Tao Huang and P. B. Mackenzie, published in the
Proceedings of the Banff Summer Institute, 1981.
- [155] S. D. Drell and T. M. Yan, Phys. Rev. Lett. **24**, 181 (1970).
- [156] G. B. West, Phys. Rev. Lett. **24** 1206 (1970).
- [157] S. J. Brodsky, R. Roskies, and R. Suaya, Phys. Rev **D8** 4574 (1973).
- [158] S. J. Brodsky and G. P. Lepage, Phys. Rev. **D24**, 2848 (1981).
- [159] Phys. Rev. **D33**, 1951 (1986).
- [160] A. Duncan and A. Mueller, Phys. Rev. **D21**, 636 (1980); Phys. Lett. **98B**, 159
(1980); A. Mueller, J. C. Collins and D. E. Soper, Ann. Rev. Nucl. Part. Sci., **37**,
383 (1987); E. Reya, Phys. Rept. **69**, 195 (1981); and A. H. Mueller, Lectures
on Perturbative QCD given at the Theoretical Advanced Study Institute, New
Haven, 1985.
- [161] S. J. Brodsky, G. P. Lepage, and S. A. A. Zaidi, Phys. Rev. **D23**, 1152 (1981).